Feature

2-D Symmetry: Theory and Filter Design Applications*

Hari C. Reddy, I-Hung Khoo, and P. K. Rajan

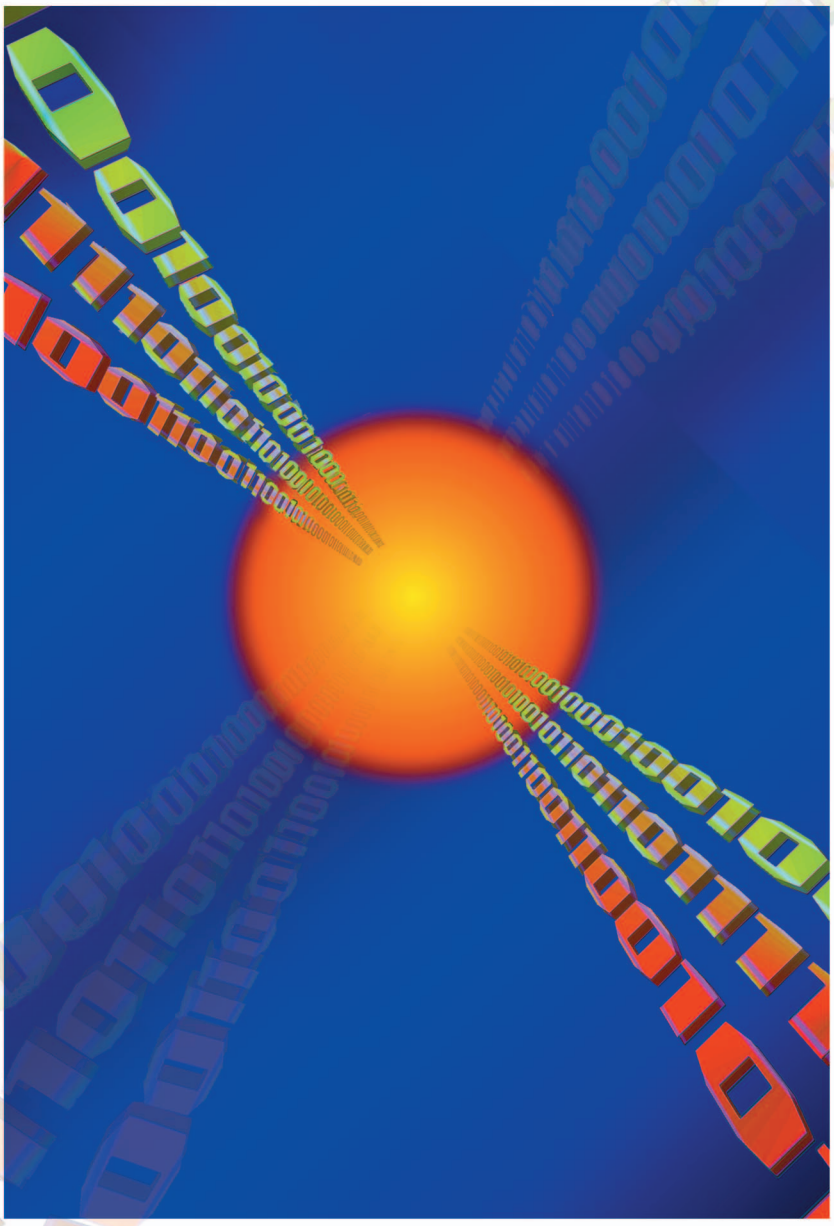

© DIGITAL STOCK

Abstract

In this comprehensive review article, we present the theory of symmetry in two-dimensional (2-D) filter functions and in 2-D Fourier transforms. It is shown that when a filter frequency response possesses symmetry, the realization problem becomes relatively simple. Further, when the frequency response has no symmetry, there is a technique to decompose that frequency response into components each of which has the desired symmetry. This again reduces the complexity of two-dimensional filter design. A number of filter design examples are illustrated.

*Paper invited for *Circuits and Systems Magazine* by Rui J. P. de Figueiredo, chair of the Editorial Advisory Board.

1540-7977/03/$17.00©2003 IEEE

Introduction

The concept of symmetry is widely applied to geometrical figures and has been the subject matter since the days of Euclid. In fact, symmetry is an important aspect of nature [1]. During the last few centuries, this concept has been applied to abstract entities such as mathematical functions [2] and also in the fields of quantum mechanics and crystallography. One dimensional systems and polynomials can only have a limited number of symmetries such as even and odd functions associated with, say, filter magnitude and phase functions, respectively. A linear two-dimensional system has a transfer function consisting of polynomials in two independent complex variables say p_1 and p_2. In a similar way, three and higher dimensional system functions can be defined in terms of three or more complex variables. These multi-dimensional functions arise from many practical engineering systems. For example, the pictorial signal in video transmission systems is characterized by its brightness function, which is a function of two spatial variables and the time variable. Other occurrences of multi-dimensional signals that have to be processed or filtered are in the areas of digital imagery for medical x-rays, and in the analysis of satellite weather photos; enhancement of television pictures from lunar and deep space probes; etc. These two- and higher-dimensional systems may possess many types of symmetries. During the past twenty years, much research has been done to reduce the complexity of the design and implementation of multi-dimensional filters/systems possessing symmetry. Since the impulse (spatio-temporal) response and the two-dimensional frequency response (2-D Fourier transform) are inter-related, it is to be assumed that the symmetry in one function will induce some form of symmetry on the other function.

The main aim of this tutorial article is to present these interdependencies and also develop conditions on 2-D filter polynomials and functions to possess important symmetries with application in mind. It will be shown that the complexity of the design and implementation could be reduced in 2-D filters, both 2-D infinite impulse response (IIR) as well as 2-D finite impulse response (FIR), by using various types of symmetries in the frequency responses of these filters [3–14]. It has been established that by using the constraints arising out of quadrantal, diagonal, four-fold rotational, and octagonal symmetries, efficient filter design algorithms could be developed [15–20]. Some of those design techniques are illustrated in the paper. In addition, the usefulness of symmetry in reducing the complexity with regard to 2-D Fast Fourier Transform (FFT) algorithm is also presented. The paper is concluded with a discussion on symmetrical decomposition of non-symmetric data and transformations. The following is the layout of the paper section by section.

In "Basic Symmetry Definitions and Understanding", a unified expression in terms of five parameters is presented to represent the various symmetries and a number of useful symmetries listed. This is followed in the section "Two-Dimensional Fourier Transform Pairs with Symmetry" by a discussion of symmetry in 2-D Fourier transform pairs. In "Symmetry and 2-D Fast Fourier Transform", the application of symmetry to speed up the fast Fourier transform calculations for signals with some symmetries is discussed. The section "Symmetry in 2-D Magnitude Response" explores symmetry in the magnitude responses of 2-D analog and digital filters and presents design techniques that effectively utilize the symmetry conditions. The application of symmetry conditions developed earlier for the design and implementation of filters whose responses do not possess any symmetries is considered in "Symmetrical Decomposition and Transformation". The final section concludes the paper with a summary of the results presented in this paper.

Basic Symmetry Definitions and Understanding

To follow the symmetry concept, let us consider a real rational function $f(x_1, x_2)$ in two independent variables x_1 and x_2. For each pair of values of x_1 and x_2, the function f assumes a unique value. This can be represented by a three-dimensional object with x_1, x_2 plane as the base with height represented by the value of the function at each point in the plane. This gives a three-dimensional object. "A thing is symmetrical if one can subject it to a certain operation and it appears exactly the same after the operation" [21]. Expanding on this definition, one may say that the function f possesses symmetry if a pair of operations, performed simultaneously, one on the vector of variables (constituting (x_1, x_2)-plane), and the other on the value or height of the function, leaves the shape of the function f undisturbed. The existence of symmetry in $f(x_1, x_2)$ implies the value of the function at (x_1, x_2) in a region is some way related to the value of the function at (x_{1T}, x_{2T}) where (x_{1T}, x_{2T}) is obtained by some operation on (x_1, x_2), this condition being satisfied at all points in the region. Using this idea, the $T - \psi$ symmetry of a function may be defined as follows [19]:

Definition: A function $f(\underline{x})$ is said to possess a $T - \psi$ symmetry over a domain D if

Hari C. Reddy is with the Department of Electrical Engineering, California State University, Long Beach, California, USA. E-mail: hreddy@csulb.edu. I-Hung Khoo is with the Department of Electrical and Computer Engineering, University of California, Irvine, California, USA. P.K. Rajan is with the Department of Electrical and Computer Engineering, Tennessee Tech University, Cookeville, Tennessee, USA.

$$\psi\left[f\left(T\left[\underline{x}\right]\right)\right] = f\left(\underline{x}\right) \text{ for all } \underline{x} \in D \tag{1}$$

where ψ is an operation on the value of $f(\underline{x})$ and T is an operation on $\underline{x}$ that maps D onto itself on a one-to-one basis. Different $T-\psi$ operations give rise to different symmetries and the symmetries derive their names, such as $x_1 = x_2$ diagonal reflection anti-symmetry, 4-fold rotational conjugate symmetry, and so on, based on the T and ψ operations.

In the $T-\psi$ symmetry definition given above, if the region D consists of all the points in the whole $\underline{x}$ domain, i.e., D = X, then the function is said to possess a global $T-\psi$ symmetry. Here, we will restrict our attention only to global $T-\psi$ symmetries and the adjective "global" will be omitted in their descriptions. We will next discuss the nature of ψ and T operations, and consider a few of the commonly found symmetries.

Nature of ψ-Operations

Of the many possible complex scalar operations, the following definition for ψ covers many useful ones:

$$\psi[f(\underline{x})] = |f(\underline{x})|e^{j(\delta \measuredangle f(\underline{x}) + \underline{\beta}^t \underline{x} + \phi)} \tag{2}$$

where $\delta = \pm 1$, $\measuredangle f(\underline{x})$ denotes the argument of $f(\underline{x})$, $\underline{\beta}$ is a (2×1) real constant vector and ϕ is a real constant. From equation (2), it may be seen that ψ does not alter the magnitude of $f(\underline{x})$. The three parameters δ, $\underline{\beta}$ and ϕ alter only the argument of $f(\underline{x})$. From this, it is evident that if a function possesses a $T-\psi$ symmetry with respect to any set of parameters (δ, $\underline{\beta}$ and ϕ) then the magnitude of the function possesses the $T-\psi_I$ symmetry, where ψ_I represents the identity operation represented by the parameters $\delta = 1$, $\underline{\beta} = 0$ and $\phi = 0$. Many of the commonly occurring symmetries have $\underline{\beta} = 0$. The term $\underline{\beta}^t$ has been included in the ψ operation to account for some of the delay type symmetries that may be present in some functions. We list in Table 1 four specific ψ-operations used in various symmetry descriptions along with the commonly used names and the proposed symbols.

Table 1.
ψ-operations and the names of the resulting symmetries.

δ	$\underline{\beta}$	ϕ	ψ-operations	Symmetry Name	Symbol
1	$\underline{0}$	0	$\psi\left[f\left(\underline{x}\right)\right] = f\left(\underline{x}\right)$	Identity symmetry	ψ_I
1	$\underline{0}$	π	$\psi\left[f\left(\underline{x}\right)\right] = -f\left(\underline{x}\right)$	Anti-symmetry	ψ_A
−1	$\underline{0}$	0	$\psi\left[f\left(\underline{x}\right)\right] = \left[f\left(\underline{x}\right)\right]^*$	Conjugate symmetry	ψ_C
−1	$\underline{0}$	π	$\psi\left[f\left(\underline{x}\right)\right] = -\left[f\left(\underline{x}\right)\right]^*$	Conjugate anti-symmetry	ψ_{CA}

Nature of T-Operations

Simple T-operations that find application in symmetry studies can be represented by the transformation (known as affine transformation in geometry):

$$T[\underline{x}] = \underline{A} \cdot \underline{x} + \underline{b} \tag{3}$$

where $\underline{A}$ is a nonsingular (2×2) real square matrix and $\underline{b}$ is a (2×1) real vector.

T is said to be an equiaffine transformation if $|\underline{A}| = \pm 1$ in which case corresponding regions in the transformed and the original domains have the same area. T is said to be a congruent transformation if the Euclidean distance between any two points in the original region is equal to that between the corresponding (image) points in the transformed region. This will be so if and only if the matrix $\underline{A}$ is orthogonal, i.e., $\underline{A} = (\underline{A}^{-1})^t$. It is to be noted that the compounding of two transformations, T_1T_2, refers to an operation T consisting of operation T_2 followed by T_1. The compounding of transformations always obey the associative law, i.e., $T_1(T_2T_3) = (T_1T_2)T_3$. In addition, if T_1 and T_2 are two nonsingular transformations, then T_1T_2 and T_2T_1 are also nonsingular transformations.

Some of the well-known T-transformations are: (i) displacement transformation; (ii) rotational transformation; and (iii) reflection transformation. In Table 2, we list a few of the basic transformations involving only reflection and rotation.

Here, $\underline{b} = \underline{0}$ and the $\underline{A}$ matrices are formed using 1 or −1 as elements on the diagonal or off the diagonal. This results in altogether eight different combinations. One of these is the identity operation $\underline{I}$, which is a trivial case. The remaining seven operations are shown in Table 2. Of these operations, only five are needed as the product of these will give the remaining two. As such, in the rest of this paper, we will use only the first five operations (i)–(v) listed in Table 2.

It is easy to see that the transformations in Table 2 are equiaffine and congruent. In addition, the following are some interesting properties:

(a) $T_1 = -T_2 = T_7 \cdot T_2$
(b) $T_3 = -T_4 = T_7 \cdot T_4$
(c) $T_1 \cdot T_2 = T_2 \cdot T_1 = -\underline{I} = T_7$
(d) $T_3 \cdot T_4 = T_4 \cdot T_3 = -\underline{I} = T_7$
(e) $T_5^2 = -\underline{I} = T_7$

Further, the T-operations can be classified by the number of cycles. A T-operation is said to be k-cyclic if k repeated T-operations on $\underline{x}$ yields the same original $\underline{x}$. That is: $T^k[\underline{x}] = \underline{x}$ or stated in another way $T^k = \underline{I}$ (where $\underline{I}$

is the identity matrix). For example, $T_1^2 = \underline{I}$ and $T_5^4 = \underline{I}$. So, operations (i)–(iv) listed in Table 2 are 2-cyclic, while (v) is 4-cyclic.

Composite Symmetry Operation and Symmetry Parameters

We now combine the T and ψ operations and define a composite symmetry operation λ as $\lambda = (T, \psi) = (\underline{A}, \underline{b}, \delta, \underline{\beta}, \phi)$ where $T[\underline{x}] = \underline{A} \cdot \underline{x} + \underline{b}$ and $\psi[f(\underline{x})] = |f(\underline{x})| e^{j(\delta \angle f(\underline{x}) + \underline{\beta}^t \underline{x} + \phi)}$.

In terms of λ, the symmetry definition can be given as

$$\lambda[f(\underline{x})] = f(\underline{x}), \quad \forall\, \underline{x} \in D \tag{4}$$

The five parameters $(\underline{A}, \underline{b}, \delta, \underline{\beta}, \phi)$ describe the symmetry operation completely and they will hereafter be called *symmetry parameters* and be used to specify the various symmetries.

Various T–ψ_I Symmetries

Employing the various T and ψ operations, one can generate various symmetries. For example, using the T-operations (i)–(v) in Table 2 and assuming the identity ψ_I, we have the following standard symmetries. (Note that the corresponding anti-symmetry, conjugate-symmetry, and conjugate-anti-symmetry can be obtained by applying the ψ_A, ψ_C, and ψ_{CA} operations respectively).

(i) Reflection about x_1-axis symmetry: $f(\underline{x}) = f(T_1[\underline{x}])$.
(ii) Reflection about x_2-axis symmetry: $f(\underline{x}) = f(T_2[\underline{x}])$.
(iii) Reflection about $x_1 = x_2$ diagonal symmetry: $f(\underline{x}) = f(T_3[\underline{x}])$.
(iv) Reflection about $x_1 = -x_2$ diagonal symmetry: $f(\underline{x}) = f(T_4[\underline{x}])$.
(v) 90° clockwise rotational symmetry: $f(\underline{x}) = f(T_5[\underline{x}])$. This also implies $f(T_5[\underline{x}]) = f(T_5^2[\underline{x}])$ and $f(T_5^2[\underline{x}]) = f(T_5^3[\underline{x}])$, through repeated substitution of $\underline{x} = T_5[\underline{x}]$.

Table 2.
Basic *T*-operations.

	$\underline{A}$	$\underline{b}$	Name of operation	Symbol
(i)	$\begin{bmatrix} 1 & 0 \\ 0 & -1 \end{bmatrix}$	$\underline{0}$	Reflection about x_1-axis	T_1
(ii)	$\begin{bmatrix} -1 & 0 \\ 0 & 1 \end{bmatrix}$	$\underline{0}$	Reflection about x_2-axis	T_2
(iii)	$\begin{bmatrix} 0 & 1 \\ 1 & 0 \end{bmatrix}$	$\underline{0}$	Reflection about $x_1 = x_2$ diagonal	T_3
(iv)	$\begin{bmatrix} 0 & -1 \\ -1 & 0 \end{bmatrix}$	$\underline{0}$	Reflection about $x_1 = -x_2$ diagonal	T_4
(v)	$\begin{bmatrix} 0 & 1 \\ -1 & 0 \end{bmatrix}$	$\underline{0}$	90° clockwise rotation about origin	T_5
(vi)	$\begin{bmatrix} 0 & -1 \\ 1 & 0 \end{bmatrix}$	$\underline{0}$	90° anti-clockwise rotation about origin	T_6
(vii)	$\begin{bmatrix} -1 & 0 \\ 0 & -1 \end{bmatrix}$	$\underline{0}$	180° rotation about origin	T_7

Table 3.
Definitions of compound T–ψ_I symmetries.

Type of Symmetry	Conditions
Quadrantal Symmetry	$f(\underline{x}) = f(T_1[\underline{x}]) = f(T_1T_2[\underline{x}]) = f(T_2[\underline{x}])$
Diagonal Symmetry	$f(\underline{x}) = f(T_3[\underline{x}]) = f(T_3T_4[\underline{x}]) = f(T_4[\underline{x}])$
Four-Fold (90°) Rotational Symmetry	$f(\underline{x}) = f(T_5[\underline{x}]) = f\left(T_5^2[\underline{x}]\right) = f\left(T_5^3[\underline{x}]\right)$
Octagonal Symmetry	$f(\underline{x}) = f(T_1[\underline{x}]) = f(T_2[\underline{x}]) = f(T_3[\underline{x}]) = f(T_4[\underline{x}]) = f(T_5[\underline{x}]) = f\left(T_5^2[\underline{x}]\right) = f\left(T_5^3[\underline{x}]\right)$

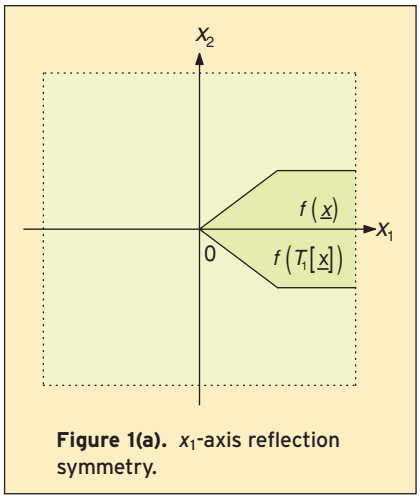

Figure 1(a). x_1-axis reflection symmetry.

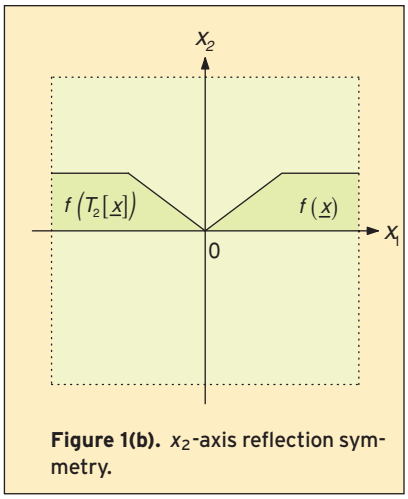

Figure 1(b). x_2-axis reflection symmetry.

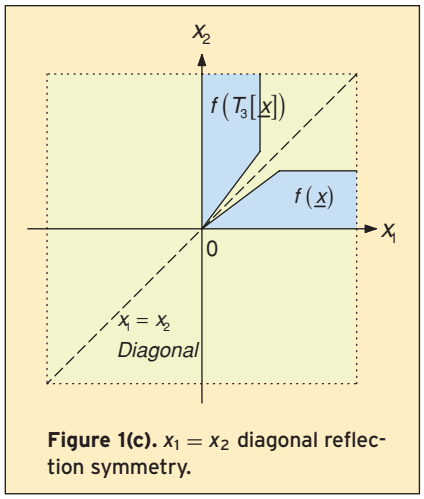

Figure 1(c). $x_1 = x_2$ diagonal reflection symmetry.

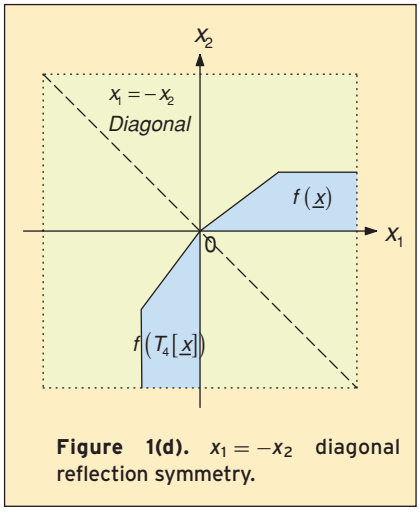

Figure 1(d). $x_1 = -x_2$ diagonal reflection symmetry.

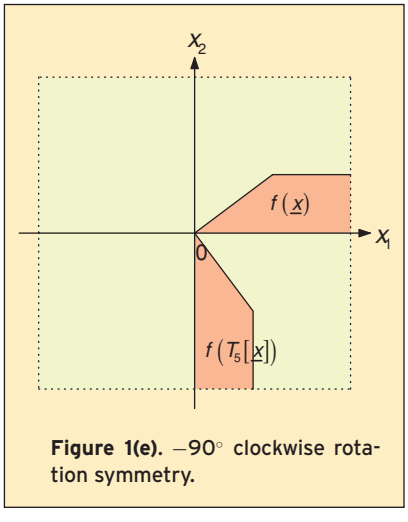

Figure 1(e). -90° clockwise rotation symmetry.

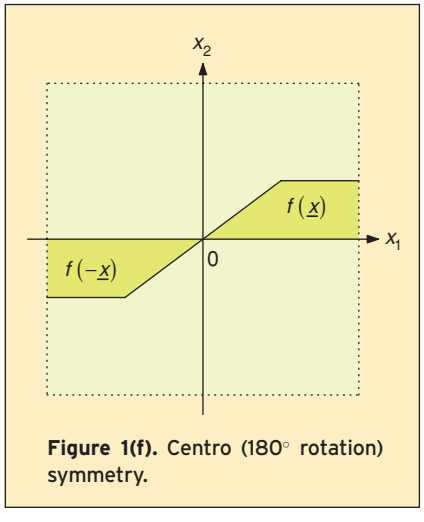

Figure 1(f). Centro (180° rotation) symmetry.

(vi) Centro (180° rotation) symmetry: $f(\underline{x}) = f(-\underline{x})$. This can also be expressed as $f(\underline{x}) = f(T_5^2[\underline{x}])$ or $f(\underline{x}) = f(T_1T_2[\underline{x}])$ or $f(\underline{x}) = f(T_3T_4[\underline{x}])$.

These symmetries are shown in Figures 1 (a)–(f). It is to be noted that the function values in the colored regions are the same, since we assumed ψ_I. For example, in Figure 1(b), the function values in the regions denoted by $f(\underline{x})$ and $f(T_2[\underline{x}])$ are the same. This is clearly the result of x_2-axis reflection symmetry.

The number of cycles in a symmetry determines the number of regions in its figure with the same function values. Reflection symmetries about x_1-axis, x_2-axis, $x_1 = x_2$ diagonal, $x_1 = -x_2$ diagonal, as well as centro symmetry, are all 2-cyclic symmetries. So they have two regions of symmetry in the X-plane. 90° clockwise rotational symmetry is 4-cyclic. So it has four regions of symmetry in the X-plane (although only two are shown in Figure 1(e)). For this reason, we usually call it four-fold (90°) rotational symmetry.

In addition to these basic symmetries, more complex symmetries can be generated using a combination of different T-operations. For example, using a combination of T_1 and T_2 operations, we can obtain quadrantal symmetry. Diagonal symmetry can be obtained using both T_3 and T_4 operations. These compound symmetries are listed in Table 3. (Once again, for illustration, we show only the symmetries resulting from the ψ_I operation.)

From "Nature of T-Operations," we can make some important observations on the compound symmetries in Table 3:

(a) Quadrantal symmetry is a combination of x_1-axis reflection, x_2-axis reflection, and centro symmetries. The presence of any two of the symmetries implies the existence of the third, i.e. $T_1 \cdot T_2 => -\underline{I}$, $-\underline{I} \cdot T_1 => T_2$, and $-\underline{I} \cdot T_2 => T_1$. So only two of the three symmetries are needed to ensure quadrantal symmetry. Also, each equation in the quadrantal symmetry condition defines a symmetry region in the X-plane. Since there are four equations in the symmetry condition, there will be four regions of symmetry in the X-plane. Finally, in terms of cycles, quadrantal symmetry is a double 2-cyclic symmetry $(T_1 \cdot T_2) \cdot (T_1 \cdot T_2) = \underline{I}$. Because of the cyclical property, the operation $T_1^m T_2^n$, where m and n are integers,

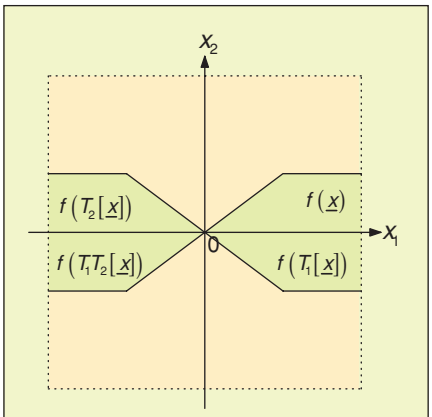

Figure 2(a). Quadrantal Symmetry.

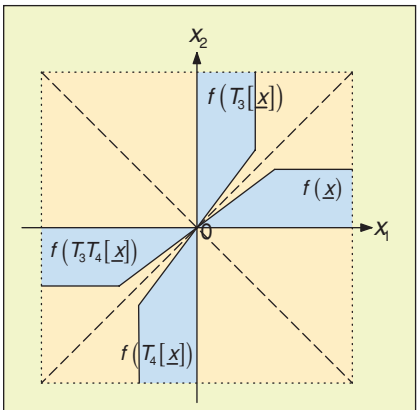

Figure 2(b). Diagonal Symmetry.

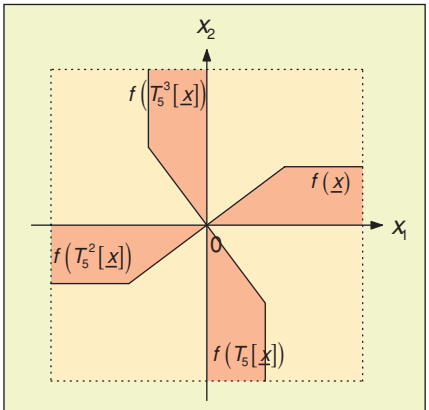

Figure 2(c). 4-fold Rotational Symmetry.

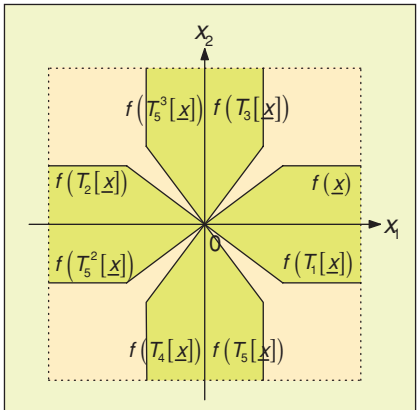

Figure 2(d). Octagonal Symmetry.

corresponds to one of the following four possibilities: $\underline{I}$, T_1T_2, T_1, or T_2.

(b) Diagonal symmetry is a combination of $x_1 = x_2$ diagonal, $x_1 = -x_2$ diagonal, and centro symmetries. The presence of any two of the three symmetries implies the existence of the third and is enough to ensure diagonal symmetry. Diagonal symmetry is a double 2-cyclic symmetry. The operation $T_3^m T_4^n$, where m and n are integers, corresponds to one of the following four possibilities: $\underline{I}$, T_3T_4, T_3, or T_4. This results in four regions of symmetry in the X-plane.

(c) Four-fold (90°) rotational symmetry is a 4-cyclic symmetry. It is formed by four repeated application of T_5. As such, there are four regions of symmetry in the X-plane for 4-fold rotational.

(d) Octagonal symmetry is a combination of quadrantal, diagonal and 4-fold rotational symmetries. The presence of any two of the three symmetries implies the existence of the third, and is sufficient to guarantee octagonal symmetry. More specifically, octagonal symmetry can result from the presence of 4-fold rotational symmetry and one of the following symmetries: x_1-axis reflection, x_2-axis reflection, $x_1 = x_2$ diagonal reflection, or $x_1 = -x_2$ diagonal reflection. So, we can classify octagonal symmetry as a combination of 4-cyclic and 2-cyclic symmetries. Alternatively, octagonal symmetry can also result from the presence of any three of the following symmetries: x_1-axis reflection, x_2-axis reflection, $x_1 = x_2$ diagonal reflection, or $x_1 = -x_2$ diagonal reflection. Thus, octagonal symmetry can also be classified as a triple 2-cyclic symmetry. Finally, since eight equations are involved in the symmetry condition, there are eight regions of symmetry in the X-plane for octagonal.

To aid in understanding, Figures 2(a)–(d) show the graphical interpretation of the quadrantal, diagonal, rotational, and octagonal symmetries. Once again, the values of the function in the colored regions are related to one another in the manner specified by the ψ operation (i.e. identity, negative, conjugate, or negative conjugate). From the figures, one should be able to confirm, as previously discussed, that there are four regions of symmetry in the X-plane for quadrantal, diagonal, and 4-fold rotational symmetries, and eight regions for octagonal symmetry. Note that

$$\begin{aligned} f(T_1T_2[\underline{x}]) &= f(T_3T_4[\underline{x}]) = f\left(T_5^2[\underline{x}]\right) \\ &= f(-\underline{x}) \end{aligned}$$

Two-Dimensional Fourier Transform Pairs with Symmetry

Two-dimensional (2-D) Fourier transform plays an important role in the analysis and design of 2-D linear systems. The transform uniquely relates the impulse or unit sample response of a linear system with its frequency response. Hence, symmetry in one response (either impulse or frequency response) may be expected to induce some form of symmetry in the other response. The existence of such symmetries can be utilized to simplify the analysis and design of these systems. Such utilization and the resulting simplification have been reported in the design and analysis of two and higher dimensional digital filters. Here, we present, in a unified manner, the type of symmetry induced in one function (Fourier transform or inverse Fourier transform) as a result of a particular symmetry in the other function for both continuous and discrete-time signals.

Continuous-Time Continuous-Frequency Case

Let $g(\underline{l}) = g(l_1, l_2)$, where l_1, l_2 are real numbers, be a two-dimensional signal and $G(\underline{\omega}) = G(j\omega_1, j\omega_2)$ be the two-dimensional Fourier transform of $g(\underline{l})$. In general, we assume $g(\underline{l})$ and $G(\underline{\omega})$ to be complex functions of real variables and $g(\underline{l})$ is such that its 2-dimensional Fourier transform $G(\underline{\omega})$ exists. If $g(\underline{l})$ is the impulse response of a stable continuous domain system, the conditions for the existence of its Fourier transform will always be satisfied. The Fourier transform pair connecting $g(\underline{l})$ and $G(\underline{\omega})$ are as follows:

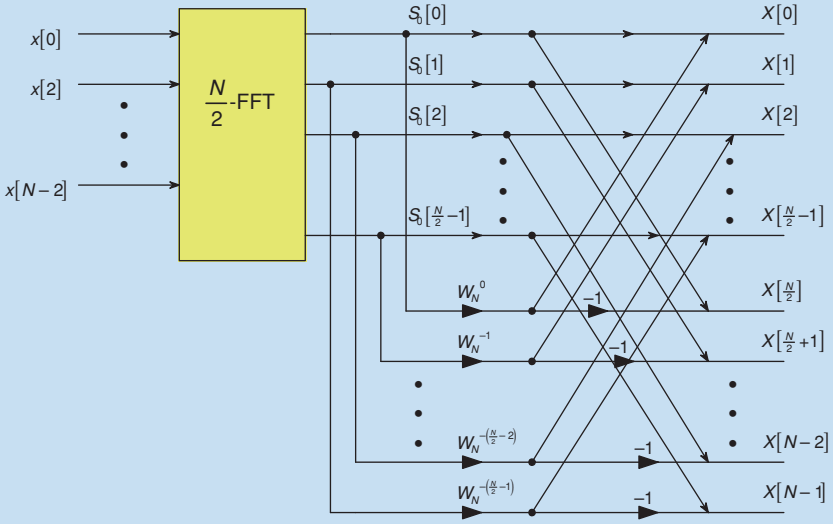

Figure 3. Symmetry-based FFT Diagram.

$$G(\underline{\omega}) = \int_{\underline{l} \in L} g(\underline{l}) \cdot e^{-j\underline{\omega}^t \underline{l}} \cdot d\underline{l} \tag{5}$$

and

$$g(\underline{l}) = \frac{1}{(2\pi)^2} \int_{\underline{\omega} \in W} G(\underline{\omega}) \cdot e^{j\underline{l}^t \underline{\omega}} \cdot d\underline{\omega} \tag{6}$$

where $d\underline{l} \triangleq dl_1 \cdot dl_2$ and $d\underline{\omega} \triangleq \omega_1 \cdot d\omega_2$.

As $g(\underline{l})$ and $G(\underline{\omega})$ are functions of 2 variables, they may possess some of the $T-\psi$ symmetries described in the section "Basic Symmetry Definitions and Understanding." We next state a theorem which gives the nature of a $T-\psi$ symmetry that will be present in $g(\underline{l})$, given a symmetry in $G(\underline{\omega})$ and vice-versa. The proof of this theorem can be found in [22].

Theorem 1: Let $g(\underline{l})$ and $G(\underline{\omega})$ form a 2-dimensional Fourier transform pair. Then $G(\underline{\omega})$ possesses a $T-\psi$ symmetry with parameters $(\underline{A}, \underline{b}, \delta, \underline{\beta}, \phi)$, $|\underline{A}| = \pm 1$, if and only if $g(\underline{l})$ possesses a $T-\psi$ symmetry with parameters $(\delta \cdot (\underline{A}^{-1})^t, \delta\underline{\beta}, \delta, -\delta\underline{b}, \underline{b}^t\underline{\beta} + \phi)$ where $\underline{A}, \underline{b}, \delta, \underline{\beta}, \phi$ are as defined in the section "Basic Symmetry Definitions and Understanding."

Observations: Next we make the following observations based on Theorem 1.

(i) If $(\underline{A}, \underline{b}, \delta, \underline{\beta}, \phi)_{\underline{\omega}}$ and $(\underline{A}, \underline{b}, \delta, \underline{\beta}, \phi)_{\underline{l}}$ are respectively the $\underline{\omega}$-domain and the $\underline{l}$-domain symmetry parameters, the corresponding $\underline{l}$ and $\underline{\omega}$ domain parameters are obtained by the following relations:

$$(\underline{A}, \underline{b}, \delta, \underline{\beta}, \phi)_{\underline{\omega}} \Rightarrow (\delta \cdot (\underline{A}^{-1})^t, \delta\underline{\beta}, \delta, -\delta\underline{b}, \underline{b}^t\underline{\beta} + \phi)_{\underline{l}} \tag{7}$$

and

$$(\underline{A}, \underline{b}, \delta, \underline{\beta}, \phi)_{\underline{l}} \Rightarrow (\delta \cdot (\underline{A}^{-1})^t, -\delta\underline{\beta}, \delta, \delta\underline{b}, \underline{b}^t\underline{\beta} + \phi)_{\underline{\omega}} \tag{8}$$

One can easily verify the compatibility of the two relations by noting that one relation is the inverse of the other relation. The reason for the appearance of the negative sign in front of $\delta\underline{b}$ in (7) whereas it is in front of $\delta\underline{\beta}$ in (8) may be attributed to the differing signs in $e^{\pm j\underline{\omega}^t\underline{l}}$ in the definitions of Fourier and inverse Fourier transforms (5) and (6).

(ii) Theorem 1 and the observation (i) also illustrate the duality present in $\underline{\omega}$ and $\underline{l}$ domain symmetries.

(iii) Further, it may be noted that the nature of symmetry transformation, such as rotation, reflection, etc., as identified by the $\underline{A}$-matrix remains the same in both the $\underline{\omega}$ and $\underline{l}$ domains.

(iv) Identical symmetries resu1t in both $\underline{\omega}$ and $\underline{l}$ domains if $\delta = 1$, $\underline{b} = 0$ and $\underline{\beta} = 0$.

We next illustrate the application of Theorem 1 using an example.

Example 1: Let $G(\underline{\omega})$ possess a centro-conjugate symmetry specified by the parameters: $(\underline{A}, \underline{b}, \delta, \underline{\beta}, \phi)_{\underline{\omega}} = \left(\begin{bmatrix} -1 & 0 \\ 0 & -1 \end{bmatrix}, \begin{bmatrix} 0 \\ 0 \end{bmatrix}, -1, \begin{bmatrix} 0 \\ 0 \end{bmatrix}, 0\right)$. Then, as per Theorem 1, the parameters of the $T-\psi$ symmetry of $g(\underline{l})$ will be $\left(\begin{bmatrix} 1 & 0 \\ 0 & 1 \end{bmatrix}, \begin{bmatrix} 0 \\ 0 \end{bmatrix}, -1, \begin{bmatrix} 0 \\ 0 \end{bmatrix}, 0\right)$. Substituting these parameters in the definition of $T-\psi$ symmetry, we get:

$$|g(\underline{l})|\, e^{j\{-\angle g(\underline{l})\}} = g(\underline{l})$$
$$\text{i.e., } [g(\underline{l})]^* = g(\underline{l})$$

or in other words $g(\underline{l})$ possesses an identity conjugate symmetry. This can only be satisfied if $g(\underline{l})$ has real coefficients.

Example 2: Let $g(\underline{l})$ possess a 4-fold rotational anti-symmetry specified by the parameters: $(\underline{A}, \underline{b}, \delta, \underline{\beta}, \phi)_{\underline{l}} = \left(\begin{bmatrix} 0 & -1 \\ 1 & 0 \end{bmatrix}, \begin{bmatrix} 0 \\ 0 \end{bmatrix}, 1, \begin{bmatrix} 0 \\ 0 \end{bmatrix}, \pi\right)$. Then, as per Theorem 1, the parameters of the $T-\psi$ symmetry of $G(\underline{\omega})$ will be $\left(\begin{bmatrix} 0 & -1 \\ 1 & 0 \end{bmatrix}, \begin{bmatrix} 0 \\ 0 \end{bmatrix}, 1, \begin{bmatrix} 0 \\ 0 \end{bmatrix}, \pi\right)$. It can be seen that $G(\underline{\omega})$ possesses the same 4-fold rotational anti-symmetry, which agrees with observation (iv).

Example 3: Let a one-dimensional signal $g(l)$ possess a translation symmetry (periodicity) specified by the parameters: $(\underline{A}, \underline{b}, \delta, \underline{\beta}, \phi)_l = ([1], [L], 1, [0], 0)$. Then, as per Theorem 1, the parameters of $T-\psi$ symmetry of $G(\underline{\omega})$ will be $([1], [0], 1, [L], 0)$. The resulting constraint on $G(\omega)$ is given by

$$G(\omega) \cdot e^{jL\omega} = G(\omega)$$

It may be noted that this equation will be satisfied only if $G(\omega) = 0$ for all ω except those discrete frequencies corresponding to $\omega_k = 2k\pi/L$. It may be noted that this corresponds to Fourier transform of periodic signals (i.e. Fourier series).

Continuous-Time Discrete-Frequency Case (Fourier Series)

Let $h(\underline{l}) = h(l_1, l_2)$ be a 2-D continuous-time periodic signal with periods L_1 and L_2, respectively in l_1 and l_2 directions. Let $H[\underline{k}] = H[k_1, k_2]$ be the two-dimensional Fourier series coefficients of $h(l_1, l_2)$. The relations between $h(\underline{l})$ and $H[\underline{k}]$ are given by

$$H[\underline{k}] = \frac{1}{L_1 \cdot L_2} \cdot \int_{l_1=0}^{L_1} \int_{l_2=0}^{L_2} h(\underline{l}) \cdot e^{-j \cdot \underline{k}^t \cdot \underline{V} \cdot \underline{l}} \cdot dl \qquad (9)$$

and

$$h(\underline{l}) = \sum_{\underline{k}} H[\underline{k}] \cdot e^{j \cdot \underline{k}^t \cdot \underline{V} \cdot \underline{l}} \qquad (10)$$

where

$$\underline{V} = \begin{bmatrix} V_1 & 0 \\ 0 & V_2 \end{bmatrix} = \begin{bmatrix} \frac{2\cdot\pi}{L_1} & 0 \\ 0 & \frac{2\cdot\pi}{L_2} \end{bmatrix}$$

represents the fundamental frequencies in the two directions. It may be verified that $h(\underline{l})$ is a doubly periodic function indicating the existence of displacement symmetries. In the following, we will consider the general $T-\psi$ symmetry relations.

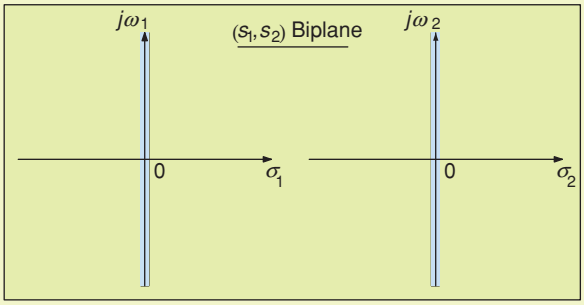

Figure 4. (s_1, s_2) biplane. (The frequency response is evaluated on the imaginary axes, $s_i = j\omega_i$.)

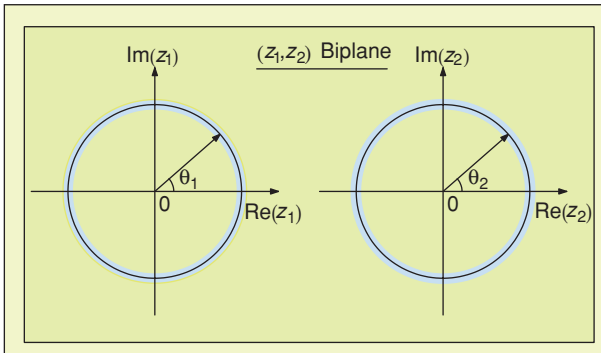

Figure 5. (z_1, z_2) biplane. (The frequency response is evaluated on the unit circles, $z_i = e^{j\theta_i}$.)

Theorem 2: Let $H[\underline{k}]$ be the Fourier series representation of a periodic function $h(\underline{l})$. Then $h(\underline{l})$ possesses a $T-\psi$ symmetry with parameters $(\underline{A}, \underline{b}, \delta, \underline{\beta}, \phi)$, $|\underline{A}| = \pm 1$, if and only if $H[\underline{k}]$ possesses a $T-\psi$ symmetry with parameters $(\delta \cdot (\underline{A}^{-1})^t, -\delta \cdot \underline{V}^{-1} \cdot \underline{\beta}, \delta, \delta \cdot \underline{V} \cdot \underline{b}, \underline{b}^t \underline{\beta} + \phi)$ where $\underline{A}, \underline{b}, \delta, \underline{\beta}, \phi$ are as defined in the section "Basic Symmetry Definitions and Understanding."

It may be noted that the overall nature of the symmetry parameters in Theorem 1 and 2 are the same except in Theorem 2, the normalizing fundamental frequency matrix appears. It should also be noted that $\underline{b}$ and $-\delta \cdot \underline{V}^{-1} \cdot \underline{\beta}$ are integer vectors. The observations made at the end of the discussions in the continuous domain case are applicable here also. Consequently, the relations between $\underline{k}$ and $\underline{l}$ domain parameters are given by

$$(\underline{A}, \underline{b}, \delta, \underline{\beta}, \phi)_{\underline{l}} \Rightarrow \left(\delta \cdot (\underline{A}^{-1})^t, -\delta \cdot \underline{V}^{-1} \cdot \underline{\beta}, \delta, \delta \cdot \underline{V} \cdot \underline{b}, \underline{b}^t \underline{\beta} + \phi\right)_{\underline{k}} \qquad (11)$$

and

$$(\underline{A}, \underline{b}, \delta, \underline{\beta}, \phi)_{\underline{k}} \Rightarrow \left(\delta \cdot (\underline{A}^{-1})^t, \delta \cdot \underline{V}^{-1} \cdot \underline{\beta}, \delta, \quad -\delta \cdot \underline{V} \cdot \underline{b}, \underline{b}^t \underline{\beta} + \phi\right)_{\underline{l}} \qquad (12)$$

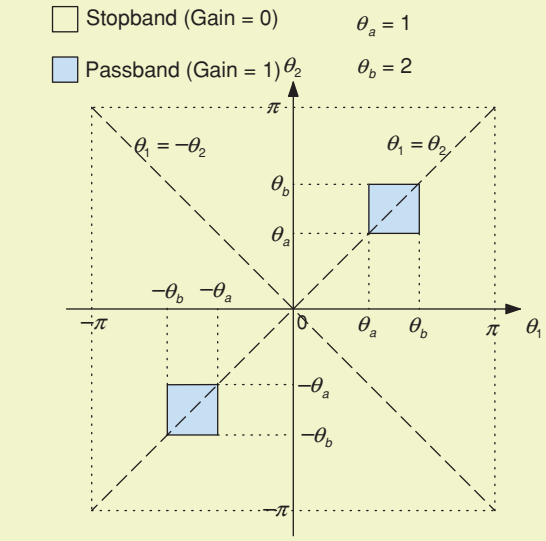

Figure 6. Specification for a bandpass filter with diagonal symmetry.

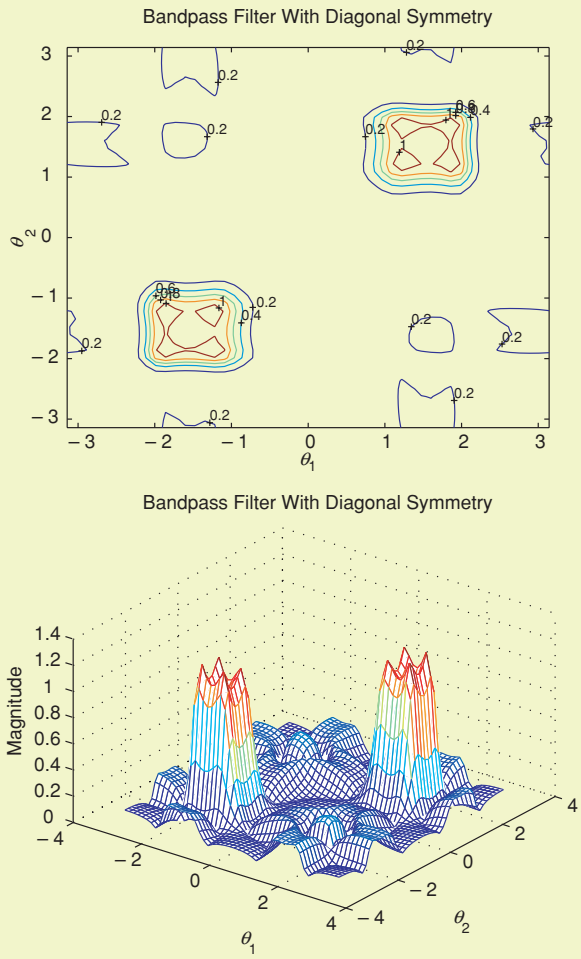

Figure 7. Contour and 3-D magnitude plots of the optimized filter with diagonal symmetry.

In the application of this theorem, it should be noted that $h(\underline{l})$ is periodic and $H[\underline{k}]$ is a discrete domain function.

Discrete-Time Continuous-Spectrum Case

Let $h(\underline{n}) = h(n_1, n_2)$, where n_1, n_2 are integers, be a two-dimensional discrete domain signal and $H(\underline{\theta}) = H(e^{-j\theta_1}, e^{-j\theta_2})$ be the two-dimensional Fourier transform of $h(\underline{n})$. When $h(\underline{n})$ represents the unit sample response of a discrete domain system, $H(\underline{\theta})$ will represent its frequency response. The Fourier transform pair connecting $h(\underline{n})$ and $H(\underline{\theta})$ are given by:

$$H(\underline{\theta}) = \sum_{\underline{n} \in N^2} h(\underline{n}) \cdot e^{-j\underline{\theta}^t \underline{n}} \tag{13}$$

and

$$h(\underline{n}) = \frac{1}{(2\pi)^2} \int_{\underline{\theta} \in \theta_p} H(\underline{\theta}) \cdot e^{j\underline{n}^t \underline{\theta}} \cdot d\underline{\theta} \tag{14}$$

where $\theta_p = \{\underline{\theta} | -\pi \le \theta_1 \le \pi, -\pi \le \theta_2 \le \pi\}$ and $d\underline{\theta} = d\theta_1 \cdot d\theta_2$.

It may easily be verified from (13) that $H(\underline{\theta})$ is a periodic function of $\underline{\theta}$ with a period of 2π in the θ_1 and θ_2 directions. As $h(\underline{n})$ and $H(\underline{\theta})$ are functions of two variables, they may possess some of the $T - \psi$ symmetries described in "Basic Symmetry Definitions and Understanding." Because of the periodic nature of $H(\underline{\theta})$, displacement symmetries in θ_1 and θ_2 directions are always present. This is due to the discrete nature of $h(\underline{n})$. We will consider the effects of the remaining symmetries that will be present in $h(\underline{n})$, given a symmetry in $H(\underline{\theta})$ and vice-versa. This is presented in the following theorem.

Theorem 3: Let $h(\underline{n})$ and $H(\underline{\theta})$ be a two-dimensional Fourier transform pair. Then $H(\underline{\theta})$ possesses a $T - \psi$ symmetry with parameters $(\underline{A}, \underline{b}, \delta, \underline{\beta}, \phi)$, $|\underline{A}| = \pm 1$, if and only if $h(\underline{n})$ possesses a $T - \psi$ symmetry with parameters $(\delta \cdot (\underline{A}^{-1})^t, \delta\underline{\beta}, \delta, -\delta\underline{b}, \underline{b}^t\underline{\beta} + \phi)$ where $\underline{A}, \underline{b}, \delta, \underline{\beta}, \phi$ are as defined in "Basic Symmetry Definitions and Understanding."

The similarity between Theorem 3 and Theorem 1 should be obvious. As such, the observations made at the end of the discussion in the continuous domain case are applicable to the discrete domain case as well. Consequently, the relations between $\underline{\theta}$ and $\underline{n}$ symmetry parameters are given by:

$$(\underline{A}, \underline{b}, \delta, \underline{\beta}, \phi)_{\underline{\theta}} \Rightarrow (\delta \cdot (\underline{A}^{-1})^t, \delta\underline{\beta}, \delta, -\delta\underline{b}, \underline{b}^t\underline{\beta} + \phi)_{\underline{n}} \tag{15}$$

and

$$(\underline{A}, \underline{b}, \delta, \underline{\beta}, \phi)_{\underline{n}} \Rightarrow (\delta \cdot (\underline{A}^{-1})^t, -\delta\underline{\beta}, \delta, \delta\underline{b}, \underline{b}^t\underline{\beta} + \phi)_{\underline{\theta}} \tag{16}$$

In the application of this theorem, it should be noted that $h(\underline{n})$ is a function of discrete domain variable $\underline{n}$ and $h(\underline{n}) = \underline{0}$ if $\underline{n}$ is not an integer vector.

Discrete-Time Discrete-Frequency Case (Discrete Fourier Transform)

Let $h[\underline{n}] = h[n_1, n_2]$ be a two-dimensional discrete-domain signal defined over $0 \le n_1 \le (N_1 - 1)$ and $0 \le n_2 \le (N_2 - 1)$. Then its (N_1, N_2) length 2-D discrete Fourier transform is given by

$$H[\underline{k}] = H[k_1, k_2] = \sum_{n_1=0}^{N_1-1} \sum_{n_2=0}^{N_2-1} h[\underline{n}] \cdot e^{-j \cdot \underline{k}^t \cdot \underline{V} \cdot \underline{n}}, \quad 0 \le k_1 \le (N_1 - 1), \quad 0 \le k_2 \le (N_2 - 1) \tag{17}$$

where

$$\underline{V} = \begin{bmatrix} \frac{2 \cdot \pi}{N_1} & 0 \\ 0 & \frac{2 \cdot \pi}{N_2} \end{bmatrix}$$

The inverse discrete Fourier transform is given by

$$h[\underline{n}] = h[n_1, n_2] = \frac{1}{N_1 \cdot N_2} \cdot \sum_{k_1=0}^{N_1-1} \sum_{k_2=0}^{N_2-1} H[\underline{k}] \cdot e^{j \cdot \underline{k}^t \cdot \underline{V} \cdot \underline{n}} \tag{18}$$

It may be noted that even though $h[n_1, n_2]$ and $H[k_1, k_2]$ are defined in the square $[0, N_1 - 1] \times [0, N_2 - 1]$, they satisfy the doubly periodic relations $h[n_1 + r_1 \cdot N_1, n_2 + r_2 \cdot N_2] = h[n_1, n_2]$ for any integer r_1 and r_2 and similarly $H[k_1 + r_1 \cdot N_1, k_2 + r_2 \cdot N_2] = H[k_1, k_2]$ for any integer r_1 and r_2. The symmetry relations between h and H are given in terms of $T - \psi$ parameters next.

Theorem 4: Let $H[\underline{k}]$ be the discrete Fourier transform of $h[\underline{n}]$. Then $h[\underline{n}]$ possesses a $T - \psi$ symmetry with parameters $(\underline{A}, \underline{b}, \delta, \underline{\beta}, \phi)$ if and only if $H[\underline{k}]$ possesses a $T - \psi$ symmetry with parameters $(\delta \cdot (\underline{A}^{-1})^t, -\delta \cdot \underline{V}^{-1} \cdot \underline{\beta}, \delta, \quad \delta \cdot \underline{V} \cdot \underline{b}, \underline{b}^t \underline{\beta} + \phi)$ where $\underline{A}, \underline{b}, \delta, \underline{\beta}, \phi$ are as defined in "Basic Symmetry Definitions and Understanding."

As in the previous cases, the symmetry parameters of $\underline{n}$ and $\underline{k}$ domains can be written as

$$(\underline{A}, \underline{b}, \delta, \underline{\beta}, \phi)_{\underline{n}} \Rightarrow (\delta \cdot (\underline{A}^{-1})^t, -\delta \cdot \underline{V}^{-1} \cdot \underline{\beta}, \delta, \delta \cdot \underline{V} \cdot \underline{b}, \underline{b}^t \underline{\beta} + \phi)_{\underline{k}} \tag{19}$$

and

$$(\underline{A}, \underline{b}, \delta, \underline{\beta}, \phi)_{\underline{k}} \Rightarrow (\delta \cdot (\underline{A}^{-1})^t, \delta \cdot \underline{V}^{-1} \cdot \underline{\beta}, \delta, -\delta \cdot \underline{V} \cdot \underline{b}, \underline{b}^t \underline{\beta} + \phi)_{\underline{n}} \tag{20}$$

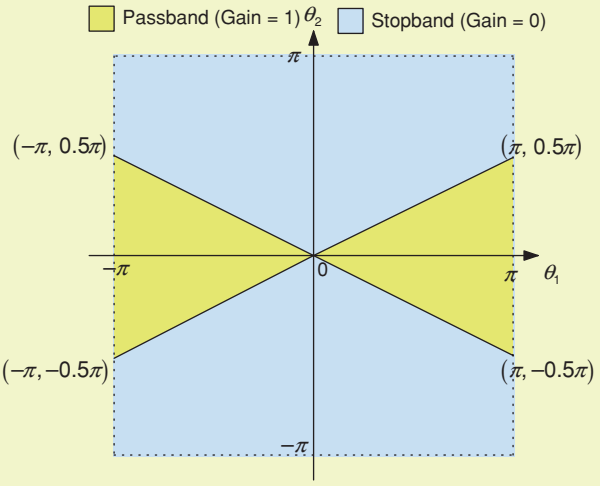

Figure 8. Specification for a fan filter with quadrantal symmetry.

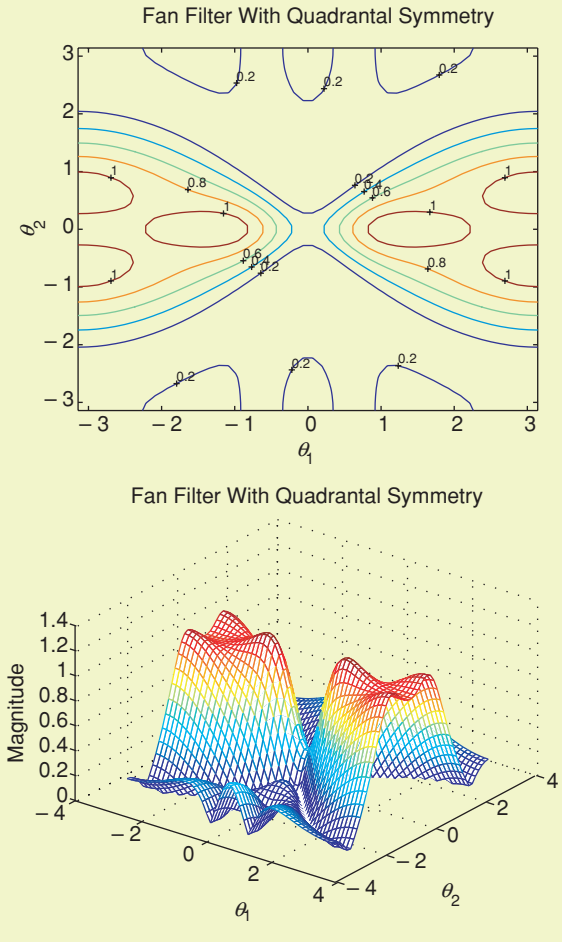

Figure 9. Contour and 3-D magnitude plots of the optimized fan filter with quadrantal symmetry.

Table 4.
Symmetries definitions for continuous and discrete domain magnitude squared functions.

Type of Symmetry	Condition on $F_C(\omega_1, \omega_2), \forall\ (\omega_1, \omega_2)$	Condition on $F_D(\theta_1, \theta_2), \forall\ (\theta_1, \theta_2)$
Quadrantal	$F_C(\omega_1, \omega_2) = F_C(-\omega_1, \omega_2) = F_C(\omega_1, -\omega_2) = F_C(-\omega_1, -\omega_2)$	$F_D(\theta_1, \theta_2) = F_D(-\theta_1, \theta_2) = F_D(\theta_1, -\theta_2) = F_D(-\theta_1, -\theta_2)$
Diagonal	$F_C(\omega_1, \omega_2) = F_C(\omega_2, \omega_1) = F_C(-\omega_1, -\omega_2) = F_C(-\omega_2, -\omega_1)$	$F_D(\theta_1, \theta_2) = F_D(\theta_2, \theta_1) = F_D(-\theta_1, -\theta_2) = F_D(-\theta_2, -\theta_1)$
Four-Fold (90°) Rotational	$F_C(\omega_1, \omega_2) = F_C(-\omega_2, \omega_1) = F_C(-\omega_1, -\omega_2) = F_C(\omega_2, -\omega_1)$	$F_D(\theta_1, \theta_2) = F_D(-\theta_2, \theta_1) = F_D(-\theta_1, -\theta_2) = F_D(\theta_2, -\theta_1)$
Octagonal	$F_C(\omega_1, \omega_2) = F_C(\omega_2, \omega_1) = F_C(-\omega_2, \omega_1) = F_C(-\omega_1, \omega_2) = F_C(-\omega_1, -\omega_2) = F_C(-\omega_2, -\omega_1) = F_C(\omega_2, -\omega_1) = F_C(\omega_1, -\omega_2)$	$F_D(\theta_1, \theta_2) = F_D(\theta_2, \theta_1) = F_D(-\theta_2, \theta_1) = F_D(-\theta_1, \theta_2) = F_D(-\theta_1, -\theta_2) = F_D(-\theta_2, -\theta_1) = F_D(\theta_2, -\theta_1) = F_D(\theta_1, -\theta_2)$

In the application of this theorem it should be noted that $\underline{n}$ and $\underline{k}$ are integer vectors and $h[\underline{n}]$ and $H[\underline{k}]$ are periodic with periods N_1 and N_2 in the two dimensions.

Symmetry and 2-D Fast Fourier Transform

Fast Fourier transform (FFT) is a frequently used operation on 2-D signals. For large size signals, it is also one of the time consuming operation. So, any technique that reduces this complexity is desirable. As noted earlier, presence of symmetry in a signal yields some constraints on the spectrum. Therefore, use of symmetry constraints can be expected to reduce the complexity of evaluation of 2-D Fourier transforms. In this section, we will see how fast Fourier transform can be made faster by the use of symmetry constraints. First we will consider 1-D signals and then we will discuss symmetry application to 2-D fast Fourier transforms.

Symmetry-Based 1-D FFT

Let $x[n]$, $n = 0, 1, \ldots, (N-1)$ be an N-length 1-D complex signal and $X[k]$, $k = 0, 1, \ldots, (N-1)$, be the N-length discrete Fourier transform (DFT) of $x[n]$. $X[k]$ is given by

$$X[k] = \sum_{n=0}^{N-1} x[n] \cdot W_N^{k \cdot n}, \quad k = 0, 1, \ldots, (N-1) \quad (21)$$

where $W_N = e^{-j\frac{2\pi}{N}}$.

The DFT requires approximately N^2 complex multiplication and N^2 complex additions. When N is a power of 2, this can be reduced to $\frac{N}{2}\log_2 N$ complex multiplications and N^2 additions using what is called Cooley-Tukey fast Fourier transform (FFT).

1-D signals may possess reflection symmetries, translation symmetries, and identity symmetries. Reflection symmetries themselves can be with respect to the point at $N/2$ or $(N-1)/2$. To illustrate the application of symmetries and the resultant reduction in the complexity, we use reflection symmetry about the point $(N-1)/2$. Application of other symmetries yields similar reductions in complexity.

If $x[n]$ possesses reflection symmetry about $n = (N-1)/2$, then $x[N-1-n] = x[n]$ for $n = 0, 1, \ldots, (N-1)$. In terms of $T - \psi$ parameters, this corresponds to $A = [-1]$, $b = [N-1]$, $\delta = 1$, $\beta = 0$ and $\phi = 0$. The corresponding symmetry parameters in DFT domain is given by

$$A_k = [-1], \quad b_k = [0], \quad \delta_k = 1, \quad \beta_k = N-1 \text{ and } \phi_k = 0,$$

which yields the symmetry relation after employing the periodic property of $X[k]$,

$$X[k] = W_N^{-k} \cdot X[N-k], \quad k = 0, 1, \ldots, (N-1) \quad (22)$$

Therefore, only half of $X[k]$ and $x[n]$ are independent and once they are known, the other half can be determined using the symmetry relation (22).

Assuming N to be even, we next show how $X[k]$ can be determined with less number of operations than the fast

Fourier transform. Using even and odd sample decomposition we can write $X[k]$ as

$$\begin{aligned} X[k] &= \sum_{\substack{n=0 \\ n \text{ even}}}^{N-1} x[n] \cdot W_N^{k \cdot n} + \sum_{\substack{n=0 \\ n \text{ odd}}}^{N-1} x[n] \cdot W_N^{k \cdot n} \\ &= \sum_{r=0}^{\frac{N}{2}-1} x[2r] \cdot W_N^{k \cdot 2r} + \sum_{r=0}^{\frac{N}{2}-1} x[2r+1] \cdot W_N^{k \cdot (2r+1)} \quad (23) \\ &= S_0[k] + W_N^k \cdot S_1[k] \end{aligned}$$

where S_0 and S_1 are $N/2$ point DFTs. Now using the symmetry properties $x[N-1-n] = x[n]$, we can write $S_1[k]$ in terms of $S_0[k]$ as

$$S_1[k] = W_N^{-2k} \cdot S_0\left[\tfrac{N}{2} - k\right] \quad (24)$$

So for $k = 0, 1, 2, \ldots, \frac{N}{2} - 1$,

$$\begin{aligned} X[k] &= S_0[k] + W_N^k \cdot W_N^{-2k} \cdot S_0\left[\tfrac{N}{2} - k\right] \\ &= S_0[k] + W_N^{-k} \cdot S_0\left[\tfrac{N}{2} - k\right] \\ X\left[\tfrac{N}{2} + k\right] &= S_0[k] - W_N^{-k} \cdot S_0\left[\tfrac{N}{2} - k\right] \quad (25) \end{aligned}$$

Thus $X[k]$ for $k = 0, 1, 2, \ldots, (N-1)$ can be determined using $N/2$ even indexed samples. This is illustrated in the flow diagram shown in Figure 3 on page 10.

It is noted that we need only one $\frac{N}{2}$-point FFT instead of the normal two. As a result, the total number of complex multiplications needed is reduced to $\frac{N}{4}\log_2\left(\frac{N}{2}\right) + \frac{N}{2}$ instead of $\frac{N}{2}\log_2 N$ in the non-symmetrical case. Thus use of symmetry results in approximately 50% reduction in the computational complexity.

2-D Symmetries

As in the 1-D case, symmetry can be utilized to reduce the computational complexity of 2-D discrete Fourier transforms. In the following, we illustrate the symmetry application for centro symmetry and quadrantal symmetry cases.

As in the 1-D case, the reflection and rotation symmetries can be defined with respect to $\left(\frac{N}{2}, \frac{N}{2}\right)$ point or $\left(\frac{N-1}{2}, \frac{N-1}{2}\right)$ point. Because of periodicity of h, the symmetries with respect to $\left(\frac{N}{2}, \frac{N}{2}\right)$ will also correspond to symmetries with respect to the origin (0, 0) for the periodically extended signal. On the other hand, with the choice of $\left(\frac{N-1}{2}, \frac{N-1}{2}\right)$ point for reflection or rotation, the various symmetries will occur for $h[\underline{n}]$ with respect to the center of the given data. In the following, $\left(\frac{N-1}{2}, \frac{N-1}{2}\right)$ is chosen in the definition of various symmetries for $h[\underline{n}]$.

Centro symmetry about $\left(\frac{N-1}{2}, \frac{N-1}{2}\right)$

An $N \times N$ array 2-D signal $x[m, n]$ is said to possess centro symmetry about $\left(\frac{N-1}{2}, \frac{N-1}{2}\right)$ if

$$x[N-1-m, N-1-n] = x[m, n] \quad \text{for} \quad 0 \le m, n \le N-1$$

The corresponding symmetry relation for its 2-D discrete Fourier transform $X[k, l]$ is given by

$$X[N-k, N-l] = W_N^{k+l} \cdot X[k, l] \quad (26)$$

Now employing the even-indexed and odd-indexed samples decomposition, $X[k, l]$ can be written as

$$\begin{aligned} X[k, l] &= S_{00}[k, l] + W_N^k \cdot S_{10}[k, l] \\ &\quad + W_N^l \cdot S_{01}[k, l] + W_N^{k+l} \cdot S_{11}[k, l] \end{aligned} \quad (27)$$

where

$$\begin{aligned} S_{00}[k, l] &= \sum_{\substack{p=0 \\ p \text{ even}}}^{\frac{N}{2}-1} \sum_{\substack{q=0 \\ q \text{ even}}}^{\frac{N}{2}-1} x[2p, 2q] \cdot W_{\frac{N}{2}}^{k \cdot p + l \cdot q} \\ S_{10}[k, l] &= \sum_{p=0}^{\frac{N}{2}-1} \sum_{q=0}^{\frac{N}{2}-1} x[2p+1, 2q] \cdot W_{\frac{N}{2}}^{k \cdot p + l \cdot q} \\ S_{01}[k, l] &= \sum_{p=0}^{\frac{N}{2}-1} \sum_{q=0}^{\frac{N}{2}-1} x[2p, 2q+1] \cdot W_{\frac{N}{2}}^{k \cdot p + l \cdot q} \\ S_{11}[k, l] &= \sum_{p=0}^{\frac{N}{2}-1} \sum_{q=0}^{\frac{N}{2}-1} x[2p+1, 2q+1] \cdot W_{\frac{N}{2}}^{k \cdot p + l \cdot q} \end{aligned}$$

Now applying the symmetry relation we can write

$$S_{01}[k, l] = W_N^{-2(k+l)} \cdot S_{10}\left[\tfrac{N}{2} - k, \tfrac{N}{2} - l\right]$$

and

$$S_{11}[k, l] = W_N^{-2(k+l)} \cdot S_{00}\left[\tfrac{N}{2} - k, \tfrac{N}{2} - l\right]$$

Then,

$$\begin{aligned} X[k, l] &= S_{00}[k, l] + W_N^k \cdot S_{10}[k, l] \\ &\quad + W_N^{-2k-l} \cdot S_{10}\left[\tfrac{N}{2} - k, \tfrac{N}{2} - l\right] \\ &\quad + W_N^{-(k+l)} \cdot S_{00}\left[\tfrac{N}{2} - k, \tfrac{N}{2} - l\right] \end{aligned} \quad (28)$$

From the above expression it is seen that when the centro symmetry relation is employed, we need to compute only two $\left(\frac{N}{2} \times \frac{N}{2}\right)$ size 2-D FFTs instead of four $\left(\frac{N}{2} \times \frac{N}{2}\right)$ size 2-D FFTs. Thus there is a 50% reduction in the computational complexity.

Quadrantal symmetry

A 2-D array $x[m, n]$ is said to possess quadrantal symmetry if the following condition is satisfied:

$$\begin{aligned} x[m, n] &= x[N-1-m, n] = x[m, N-1-n] \\ &= x[N-1-m, N-1-n] \end{aligned} \quad (29)$$

Table 5.
Spectral forms of magnitude squared function for various symmetries.

Continuous domain	Discrete domain (Note that $x_i = z_i + z_i^{-1}$ and $y_i = z_i - z_i^{-1}$, $i = 1, 2$)
Centro Symmetry $P(s_1, s_2) \cdot P(-s_1, -s_2) = \sum_{i=0}^{m_1}\sum_{j=0}^{n_1} a_{ij} s_1^{2i} s_2^{2j} + s_1 s_2 \sum_{i=0}^{m_2}\sum_{j=0}^{n_2} b_{ij} s_1^{2i} s_2^{2j}$	**Centro Symmetry** $Q(z_1, z_2) \cdot Q(z_1^{-1}, z_2^{-1}) = \sum_{i=0}^{m_1}\sum_{j=0}^{n_1} c_{ij} x_1^i x_2^j + y_1 y_2 \sum_{i=0}^{m_2}\sum_{j=0}^{n_2} d_{ij} x_1^i x_2^j$
Quadrantal Symmetry $P(s_1, s_2) \cdot P(-s_1, -s_2) = \sum_{i=0}^{m_1}\sum_{j=0}^{n_1} a_{ij} s_1^{2i} s_2^{2j}$	**Quadrantal Symmetry** $Q(z_1, z_2) \cdot Q(z_1^{-1}, z_2^{-1}) = \sum_{i=0}^{m_1}\sum_{j=0}^{n_1} c_{ij} x_1^i x_2^j$
Diagonal Symmetry $P(s_1, s_2) \cdot P(-s_1, -s_2) = \sum_{i=0}^{m_1}\sum_{j=0}^{n_1} a_{ij} s_1^{2i} s_2^{2j} + s_1 s_2 \sum_{i=0}^{m_2}\sum_{j=0}^{n_2} b_{ij} s_1^{2i} s_2^{2j}$ where $a_{ij} = a_{ji}$ and $b_{ij} = b_{ji}$.	**Diagonal Symmetry** $Q(z_1, z_2) \cdot Q(z_1^{-1}, z_2^{-1}) = \sum_{i=0}^{m_1}\sum_{j=0}^{n_1} c_{ij} x_1^i x_2^j + y_1 y_2 \sum_{i=0}^{m_2}\sum_{j=0}^{n_2} d_{ij} x_1^i x_2^j$ where $c_{ij} = c_{ji}$ and $d_{ij} = d_{ji}$.
Four-Fold (90°) Rotational Symmetry $P(s_1, s_2) \cdot P(-s_1, -s_2) = \sum_{i=0}^{m_1}\sum_{j=0}^{n_1} a_{ij} s_1^{2i} s_2^{2j} + s_1 s_2 \sum_{i=0}^{m_2}\sum_{j=0}^{n_2} b_{ij} s_1^{2i} s_2^{2j}$ where $a_{ij} = a_{ji}$ and $b_{ij} = -b_{ji}$.	**Four-Fold (90°) Rotational Symmetry** $Q(z_1, z_2) \cdot Q(z_1^{-1}, z_2^{-1}) = \sum_{i=0}^{m_1}\sum_{j=0}^{n_1} c_{ij} x_1^i x_2^j + y_1 y_2 \sum_{i=0}^{m_2}\sum_{j=0}^{n_2} d_{ij} x_1^i x_2^j$ where $c_{ij} = c_{ji}$ and $d_{ij} = -d_{ji}$.
Octagonal Symmetry $P(s_1, s_2) \cdot P(-s_1, -s_2) = \sum_{i=0}^{m_1}\sum_{j=0}^{n_1} a_{ij} s_1^{2i} s_2^{2j}$ where $a_{ij} = a_{ji}$.	**Octagonal Symmetry** $Q(z_1, z_2) \cdot Q(z_1^{-1}, z_2^{-1}) = \sum_{i=0}^{m_1}\sum_{j=0}^{n_1} c_{ij} x_1^i x_2^j$ where $c_{ij} = c_{ji}$.

It may be noted that quadrantal symmetry is defined here with respect to the center of the array, $(\frac{N-1}{2}, \frac{N-1}{2})$. In the expression (29) for $X[k, l]$, $S_{10}[k, l]$, $S_{01}[k, l]$ and $S_{11}[k, l]$ can be expressed in terms of $S_{00}[k, l]$ as shown next.

$$\begin{aligned} S_{10}[k, l] &= \sum_{p=0}^{\frac{N}{2}-1}\sum_{q=0}^{\frac{N}{2}-1} x[2p+1, 2q] \cdot W_{\frac{N}{2}}^{p\cdot k + q\cdot l} \\ &= W_N^{-2k} \cdot S_{00}\left[\tfrac{N}{2} - k, l\right] \\ S_{01}[k, l] &= W_N^{-2l} \cdot S_{00}\left[k, \tfrac{N}{2} - l\right] \end{aligned}$$

and

$$S_{11}[k, l] = W_N^{-2(k+l)} \cdot S_{00}\left[\tfrac{N}{2} - k, \tfrac{N}{2} - l\right]$$

Then $X[k, l]$ can be written in terms of S_{00} solely as

$$\begin{aligned} X[k, l] &= S_{00}[k, l] + W_N^{-k} \cdot S_{00}\left[\tfrac{N}{2} - k, l\right] \\ &+ W_N^{-l} \cdot S_{00}\left[k, \tfrac{N}{2} - l\right] \\ &+ W_N^{-(k+l)} \cdot S_{00}\left[\tfrac{N}{2} - k, \tfrac{N}{2} - l\right] \end{aligned} \quad (30)$$

It is then noted that evaluation of $X[k, l]$ require the evaluation of four $\frac{N}{2} \times \frac{N}{2}$ size 2-D FFT's when $x[m, n]$ does not possess any symmetry whereas only one $\frac{N}{2} \times \frac{N}{2}$ size 2-D FFT is required when the quadrantal symmetry is present in $x[m, n]$. In other words, utilization of the quadrantal symmetry in $x[m, n]$ reduces the computational complexity by approximately 75%. It may also be noted that quadrantal symmetry in $x[m, n]$ as defined in (29) results in a form of quadrantal symmetry in $X[k, l]$ as

$$\begin{aligned} X[k, l] &= W_N^{-k} \cdot X[N - k, l] = W_N^{-l} \cdot X[k, N - l] \\ &= W_N^{-(k+l)} \cdot X[N - k, N - l] \end{aligned} \quad (31)$$

Symmetrical Decomposition For Data Without Symmetry

In many situations, signals do not possess any symmetries. In those cases, symmetry results cannot be applied if we process the signals as they are. One way of dealing with this situation is to decompose the signal into signals possessing symmetries and anti-symmetries. For example, $x[m, n]$ can be decomposed as

$$\begin{aligned} x[m, n] &= x_{00}[m, n] + x_{10}[m, n] \\ &+ x_{01}[m, n] + x_{11}[m, n] \end{aligned} \quad (32)$$

where x_{00} possesses quadrantal symmetry, x_{10} possesses quadrantal anti-symmetry of type 1 (anti-symmetry w.r.t. m and symmetry w.r.t. n), x_{01} possesses quadrantal anti-symmetry of type 2 (symmetry w.r.t. m and anti-symmetry w.r.t. n), and x_{11} possesses quadrantal anti-symmetry of type 3 (anti-symmetry w.r.t. both m and n).

Then each component can be processed using appropriate symmetry properties. While this method may not

reduce the overall complexity, it will facilitate parallel processing of major computations.

Symmetry in 2-D Magnitude Response

In the design of two-dimensional filters, the design specifications are usually given in terms of the magnitude spectrum which possesses certain symmetries, while the phase characteristic is either not known or is not important. In such cases, it is desirable to know the types of transfer functions that can support the specified symmetry in the magnitude response. In this section, we will present the constraints on the numerator and denominator polynomials of the transfer function, in order for them to possess the required symmetry and stability.

2-D Magnitude Response—Continuous and Discrete

Recall that the ψ operation only affects the phase of the frequency response and not the magnitude. Hence, when dealing with magnitude symmetry, we assume $\psi = \psi_I$ and call our $T - \psi$ symmetry as simply T-symmetry. Now, in order for the magnitude response of a transfer function to possess a particularly symmetry, both the numerator and denominator polynomials have to possess the symmetry individually. In other words, when studying the symmetry constraints on the transfer function, one need only focus on the polynomial symmetry constraints on the numerator and denominator. This observation is a consequence of the following theorem.

Theorem 5: Let $F_C(\underline{\omega}) = P(\underline{\omega})/D(\underline{\omega})$ be a magnitude squared function where $P(\underline{\omega})$ and $D(\underline{\omega})$ are relatively prime polynomials. If $F_C(\underline{\omega})$ possesses a $T-$symmetry, then $P(\underline{\omega})$ and $D(\underline{\omega})$ should possess the same T-symmetry individually.

It is to be noted that Theorem 5 also holds for discrete-domain cases, with appropriate change of variables.

Continuous-domain magnitude response

Let $P(s_1, s_2)$ be a continuous domain polynomial. Then its frequency response $P(j\omega_1, j\omega_2)$ is obtained by evaluating the polynomial on the imaginary axes of the (s_1, s_2) biplane as shown in Figure 4 on page 11. Here, ω_1 and ω_2 denote the real frequency variables in the two-dimensional frequency plane: $W^2 = W_1 \times W_2$.

If $P(s_1, s_2)$ only has real coefficients, then the magnitude-squared function $F_C(\omega_1, \omega_2)$, defined over the entire W^2 plane, is given by:

$$\begin{aligned} F_C(\omega_1, \omega_2) &= |P(j\omega_1, j\omega_2)|^2 \\ &= P(j\omega_1, j\omega_2) \cdot P(-j\omega_1, -j\omega_2) \end{aligned} \tag{33}$$

From (33), it is easy to see that the magnitude squared function is an even function in both ω_1 and ω_2, i.e. $F_C(\omega_1, \omega_2) = F_C(-\omega_1, -\omega_2)$. So it should always be expressible as the following general form:

$$F_C(\omega_1, \omega_2) = F_{C1}\left(\omega_1^2, \omega_2^2\right) + \omega_1\omega_2 F_{C2}\left(\omega_1^2, \omega_2^2\right) \tag{34}$$

Applying analytic continuation to (33) and (34), we can write:

$$P(s_1, s_2) \cdot P(-s_1, -s_2) = F_{C1}\left(s_1^2, s_2^2\right) + s_1 s_2 F_{C2}\left(s_1^2, s_2^2\right) \tag{35}$$

One can observe that the magnitude squared function is a rational function in s_1 and s_2. This is the reason why we choose to work with the magnitude squared function rather than the magnitude function which is not rational.

Discrete-domain magnitude response

For the discrete domain case, assuming that the polynomial is $Q(z_1, z_2)$, its frequency response $Q(e^{-j\theta_1}, e^{-j\theta_2})$ is obtained by evaluating the polynomial on the boundary of the unit circles in the (z_1, z_2) biplane as shown in Figure 5 on page 11. The discrete-domain frequency variables θ_1 and θ_2 are related to the continuous-domain ones through $\theta_1 = \omega_1 \cdot T$ and $\theta_2 = \omega_2 \cdot T$, where T is the sampling period in both directions.

If $Q(z_1, z_2)$ possesses only real coefficients, then the magnitude-squared function $F_D(\theta_1, \theta_2)$ is obtained by:

$$\begin{aligned} F_D(\theta_1, \theta_2) &= |Q(e^{-j\theta_1}, e^{-j\theta_2})|^2 \\ &= Q(e^{-j\theta_1}, e^{-j\theta_2}) \cdot Q(e^{j\theta_1}, e^{j\theta_2}) \end{aligned} \tag{36}$$

Once again, it is easy to see that the magnitude squared function is an even function, i.e. $F_D(\theta_1, \theta_2) = F_D(-\theta_1, -\theta_2)$. As such, it should be expressible as:

$$\begin{aligned} F_D(\theta_1, \theta_2) =& F_{D1}(\cos\theta_1, \cos\theta_2) \\ &+ \sin\theta_1 \cdot \sin\theta_2 \cdot F_{D2}(\cos\theta_1, \cos\theta_2) \end{aligned} \tag{37}$$

It should be obvious that, in the above, $\cos(\theta_i)$ is even and $\sin(\theta_i)$ is odd.

Using analytic continuation, we have:

$$\begin{aligned} &Q(z_1, z_2) \cdot Q\left(z_1^{-1}, z_2^{-1}\right) \\ &\quad = F_{D1}\left(z_1 + z_1^{-1}, z_2 + z_2^{-1}\right) + \left(z_1 - z_1^{-1}\right) \cdot \left(z_2 - z_2^{-1}\right) \\ &\qquad \cdot F_{D2}\left(z_1 + z_1^{-1}, z_2 + z_2^{-1}\right) \end{aligned} \tag{38}$$

Equations (35) and (38) give the spectral forms of the magnitude squared functions for the continuous domain and discrete domain cases respectively.

Bilinear transformation between 2-D continuous and discrete variables

The double bilinear transformation $s_i = (1 - z_i)/(1 + z_i)$, $i = 1, 2$ is often used to generate a 2-D discrete domain function from a 2-D continuous domain function. The advantage of this method is that the symmetry present in

the continuous domain magnitude response is carried over to the discrete domain magnitude response. The following is a simple proof. Assume,

$$F_D(z_1, z_2) = F_C(s_1, s_2)|_{s_i=(1-z_i)/(1+z_i)}, i = 1, 2$$

In terms of the frequency variables, this can be expressed as:

$$F_D(\theta_1, \theta_2) = F(\omega_1, \omega_2)|_{\omega_i=\tan(\theta_i/2)}, i = 1, 2$$

Now if $F_C(s_1, s_2)$ possesses, say, 4-fold rational symmetry, then

$$F_C(\omega_1, \omega_2) \equiv F_C(-\omega_2, \omega_1)$$

So,

$$\begin{aligned} F_D(\theta_1, \theta_2) &\equiv F_C(-\tan(\theta_2/2), \tan(\theta_1/2)) \\ &\equiv F_D(-\theta_2, \theta_1) \end{aligned}$$

Therefore, the discrete domain magnitude squared function obtained through bilinear transformation possesses the same 4-fold rational symmetry present in the original continuous domain function. It can be shown that this result holds for the other symmetries as well. We summarize in Table 4 on page 14 the symmetry conditions for our magnitude squared functions in both continuous and discrete domains.

Spectral Forms

In this section, we present the constraints on the magnitude squared function in order for it to possess the various symmetries. Recall that for a continuous or discrete domain transfer function with real coefficients, its magnitude squared function is always an even function. Focusing on the continuous domain case, this means $F_C(\omega_1, \omega_2) = F_C(-\omega_1, -\omega_2)$. As such, the magnitude squared function always possesses centro symmetry, and is expressible as (34). Now, if $F_C(\omega_1, \omega_2)$ also possesses quadrantal symmetry, then $F_C(\omega_1, \omega_2) = F_C(\omega_1, -\omega_2)$. Using (34), this can be written as:

$$\begin{aligned} &F_{C1}(\omega_1^2, \omega_2^2) + \omega_1\omega_2 F_{C2}(\omega_1^2, \omega_2^2) \\ &\quad = F_{C1}(\omega_1^2, \omega_2^2) - \omega_1\omega_2 F_{C2}(\omega_1^2, \omega_2^2) \end{aligned} \quad (39)$$

The above is only possible if $F_{C2}(\omega_1^2, \omega_2^2) = 0$. Thus, $F_C(\omega_1, \omega_2) = F_{C1}(\omega_1^2, \omega_2^2)$. So the spectral form for the magnitude squared function that possesses quadrantal symmetry is:

$$\begin{aligned} P(s_1, s_2) \cdot P(-s_1, -s_2) &= F_{C1}(s_1^2, s_2^2) \\ &= \sum_{i=0}^{m_1} \sum_{j=0}^{n_1} a_{ij} s_1^{2i} s_2^{2j} \end{aligned} \quad (40)$$

We can use the same procedure to obtain the spectral forms for the other symmetries in continuous as well as discrete domains. These spectral forms are listed in Table 5 on page 16.

Polynomial Symmetry

In order for a transfer function to possess various magnitude symmetries, the numerator and denominator polynomials have to possess the same symmetries individually. So, we now consider the symmetry constraints on the polynomials. We first introduce the following key theorem:

Theorem 6 (Unique factorization theorem for multivariable polynomial) [23]: A multivariable polynomial can be factored into a set of irreducible polynomials and the factors are unique within a multiplicative constant. In other words, let $P(\omega)$ be factored in two ways as the left-, and right-hand sides of the following identity:

$$K_1 \prod_{i=1}^{I_1} P_i(\omega) \equiv K_2 \prod_{i=1}^{I_2} Q_i(\omega)$$

where all $P_i(\omega)$'s and $Q_i(\omega)$'s are irreducible polynomials. Then, it is required that $I_1 = I_2 = I$ and for each $P_i(\omega)$, $i = 1, 2, \ldots, I$, there exists a unique $Q_j(\omega)$ (i may be equal to j) such that

$$P_i(\omega) = k_j Q_j(\omega)$$

where k_j's are constants such that $K_2 = K_1 \prod_{j=1}^{I} k_j$.

Using the unique factorization theorem, we can obtain the polynomial factors that satisfy the various symmetries. For example, for quadrantal symmetry, its magnitude squared function has to satisfy $F_C(\omega_1, \omega_2) = F_C(\omega_1, -\omega_2)$, i.e.

$$P(j\omega_1, j\omega_2) \cdot P(-j\omega_1, -j\omega_2) = P(j\omega_1, -j\omega_2) \cdot P(-j\omega_1, j\omega_2)$$

Using analytic continuation, this becomes:

$$P(s_1, s_2) \cdot P(-s_1, -s_2) = P(s_1, -s_2) \cdot P(-s_1, s_2) \quad (41)$$

If we assume $P(s_1, s_2)$ to be irreducible, the unique factorization theorem of multivariable polynomials states that $P(s_1, s_2)$ should satisfy one of the following two conditions:

(i) $P(s_1, s_2) = k_1 \cdot P(s_1, -s_2)$ where k_1 is a real constant. (42)

(ii) $P(s_1, s_2) = k_2 \cdot P(-s_1, s_2)$ where k_2 is a real constant. (43)

It is easy to see that for case (i), P needs to be even in s_2, and for case (ii), P needs to be even in s_1. Therefore, the

Table 6.
Continuous and discrete domain polynomial factors possessing symmetry.

Continuous domain	Discrete domain (Note that $x_i = z_i + z_i^{-1}$ and $y_i = z_i - z_i^{-1}$ for $i = 1, 2$)
Quadrantal Symmetry	Quadrantal Symmetry
a) $P(s_1, s_2^2)$	a) $Q(z_1, x_2)$
b) $P(s_1^2, s_2)$	b) $Q(x_1, z_2)$
c) $P(s_1, s_2) \cdot P(s_1, -s_2)$	c) $Q(z_1, z_2) \cdot Q(z_1, z_2^{-1})$
d) $P(s_1, s_2) \cdot P(-s_1, s_2)$	d) $Q(z_1, z_2) \cdot Q(z_1^{-1}, z_2)$
Diagonal Symmetry	Diagonal Symmetry
a) $P_1(s_1, s_2)$	a) $Q_1(z_1, z_2)$
b) $P_2(s_1^2, s_2^2) + s_1 s_2 P_3(s_1^2, s_2^2)$ $+ s_1 P_4(s_1^2, s_2^2) - s_2 P_4(s_2^2, s_1^2)$	b) $Q_2(x_1, x_2) + y_1 y_2 Q_3(x_1, x_2) + y_1 Q_4(x_1, x_2)$ $- y_2 Q_4(x_2, x_1)$
c) $P(s_1, s_2) \cdot P(s_2, s_1)$	c) $Q(z_1, z_2) \cdot Q(z_2, z_1)$
d) $P(s_1, s_2) \cdot P(-s_2, -s_1)$	d) $Q(z_1, z_2) \cdot Q(z_2^{-1}, z_1^{-1})$
where	where
$P_1(s_1, s_2) = P_1(s_2, s_1)$ and	$Q_1(z_1, z_2) = Q_1(z_2, z_1)$ and
$P_k(s_1^2, s_2^2) = P_k(s_2^2, s_1^2)$ for k = 2, 3.	$Q_k(x_1, x_2) = Q_k(x_2, x_1)$ for $k = 2, 3$.
Four-Fold (90°) Rotational Symmetry	Four-Fold (90°) Rotational Symmetry
a) $P_1(s_1^2, s_2^2) + s_1 s_2 \cdot (s_1^2 - s_2^2) \cdot P_2(s_1^2, s_2^2)$	a) $Q_1(x_1, x_2) + y_1 y_2 \cdot (x_1 - x_2) \cdot Q_2(x_1, x_2)$
b) $(s_1^2 - s_2^2) P_1(s_1^2, s_2^2) + s_1 s_2 P_2(s_1^2, s_2^2)$	b) $(x_1 - x_2) Q_1(x_1, x_2) + y_1 y_2 Q_2(x_1, x_2)$
c) $P(s_1, s_2) \cdot P(-s_2, s_1)$	c) $Q(z_1, z_2) \cdot Q(z_2^{-1}, z_1)$
d) $P(s_1, s_2) \cdot P(s_2, -s_1)$	d) $Q(z_1, z_2) \cdot Q(z_2, z_1^{-1})$
e) $P(s_1, s_2) \cdot P(-s_2, s_1)$ $\times P(-s_1, -s_2) \cdot P(s_2, -s_1)$	e) $Q(z_1, z_2) \cdot Q(z_2^{-1}, z_1)$ $\times Q(z_1^{-1}, z_2^{-1}) \cdot Q(z_2, z_1^{-1})$
where	where
$P_k(s_1^2, s_2^2) = P_k(s_2^2, s_1^2)$ for k = 1, 2.	$Q_k(x_1, x_2) = Q_k(x_2, x_1)$ for k = 1, 2.
Octagonal Symmetry	Octagonal Symmetry
a) $(s_1^2 - s_2^2)^\alpha \cdot P_1(s_1^2, s_2^2)$, where $\alpha = 0$ or 1.	a) $(x_1 - x_2)^\alpha \cdot Q_1(x_1, x_2)$, where $\alpha = 0$ or 1.
b) $P(s_1^2, s_2) \cdot P(s_2^2, s_1)$	b) $Q(x_1, z_2) \cdot Q(x_2, z_1)$
c) $P(s_1^2, s_2) \cdot P(s_2^2, -s_1)$	c) $Q(x_1, z_2) \cdot Q(x_2, z_1^{-1})$
d) $P(s_1, s_2^2) \cdot P(-s_2, s_1^2)$	d) $Q(z_1, x_2) \cdot Q(z_2^{-1}, x_1)$
e) $P_2(s_1, s_2) \cdot P_2(-s_1, s_2)$	e) $Q_2(z_1, z_2) \cdot Q_2(z_1^{-1}, z_2)$
f) $P_2(s_1, s_2) \cdot P_2(s_1, -s_2)$	f) $Q_2(z_1, z_2) \cdot Q_2(z_1, z_2^{-1})$
where	where
$P_1(s_1^2, s_2^2) = P_1(s_2^2, s_1^2)$ and	$Q_1(x_1, x_2) = Q_1(x_2, x_1)$ and
$P_2(s_1, s_2) = P_2(s_2, s_1)$.	$Q_2(z_1, z_2) = Q_2(z_2, z_1)$.

polynomial factors satisfying quadrantal symmetry are: $P(s_1, s_2^2)$ and $P(s_1^2, s_2)$. More factors can be derived if we assume P to be reducible. These are $P(s_1, s_2) \cdot P(s_1, -s_2)$ and $P(s_1, s_2) \cdot P(-s_1, s_2)$.

In Table 6 above we state the continuous and discrete domain polynomial factors that posses the various symmetries. These factors are derived using the procedure just discussed. It is to be noted that for the polynomial factors listed under each symmetry, their products possess the same symmetry as well. For example, $P_1(s_1, s_2^2)$ and $P_2(s_1^2, s_2)$ each possess quadrantal symmetry. So their product $P_1(s_1, s_2^2) \cdot P_2(s_1^2, s_2)$ possesses quadrantal symmetry as well.

Symmetry and Stability

For a transfer function to possess symmetry, the denom-

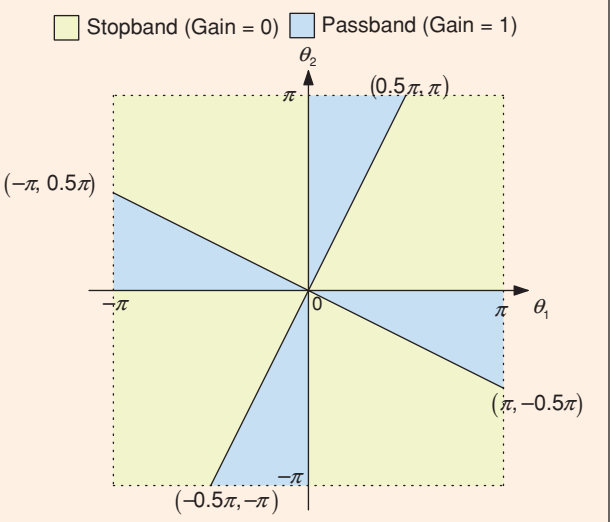

Figure 10. Specification for a fan filter with 4-fold (90°) rotational symmetry.

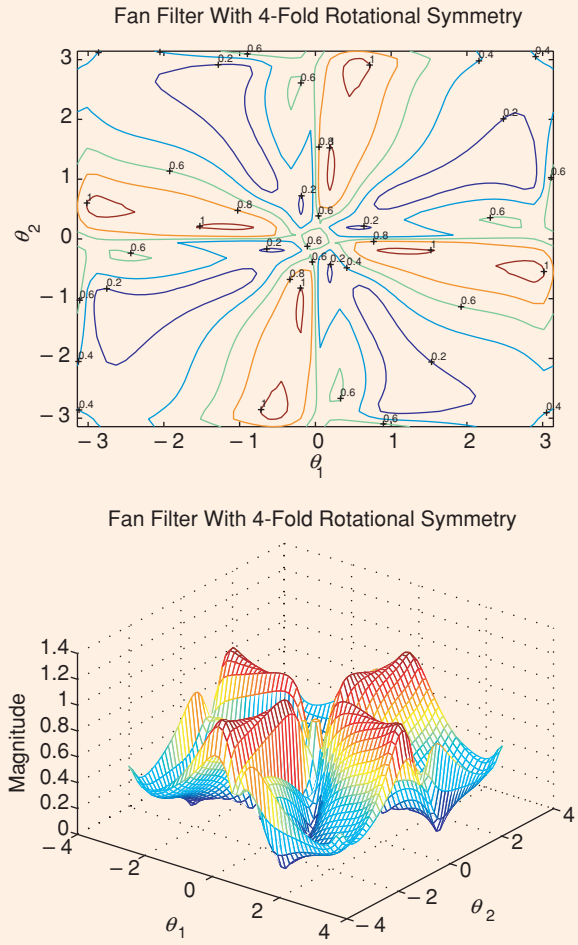

Figure 11. Contour and 3-D magnitude plots of the optimized fan filter with 4-fold rotational symmetry.

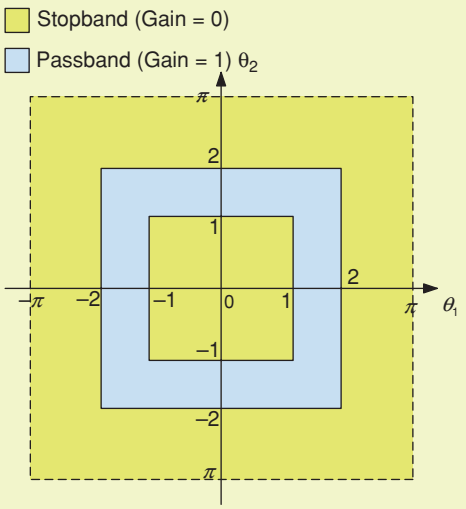

Figure 12. Specification for a bandpass filter with octagonal symmetry.

inator polynomial $D(s_1, s_2)$ has to satisfy the conditions for the symmetry as well as stability. So there is an additional stability constraint on the denominator polynomial compared to the numerator polynomial. It has been shown in [17, 24–26] that the sufficient condition for 2-D continuous domain filters to be stable is that their transfer functions do not have any poles in the region of the (s_1, s_2) biplane defined by $\mathrm{Re}(s_1) \geq 0$ and $\mathrm{Re}(s_2) \geq 0$, including infinite distant points. Similarly, a sufficient condition for the stability of 2-D discrete domain filters is that their transfer functions do not have any poles in the region of the (z_1, z_2) biplane defined by $|z_1| \leq 1$ and $|z_2| \leq 1$. Continuous domain and discrete domain stability results are related by the double bilinear transformation, $s_i = (1 - z_i)/(1 + z_i)$, $i = 1, 2$. Applying these stability conditions on the polynomial factors that possess the various magnitude symmetries, the conditions on the denominator polynomials of 2-D filters are obtained. These are listed in Table 7 on page 25. The interested reader may refer to [20] for the details and the proof.

IIR Filter Design

The design of filters involves the determination of the filter coefficients such that the resulting magnitude response approximates the ideal specifications to a certain tolerance. Design of 2-D digital filters is more complicated than 1-D digital filters because the increase in dimension brings about an exponential increase in the number of coefficients. Fortunately, 2-D frequency responses possess many types of symmetries and the presence of these symmetries can be used to reduce the complexity of the design. Symmetry present in the fre-

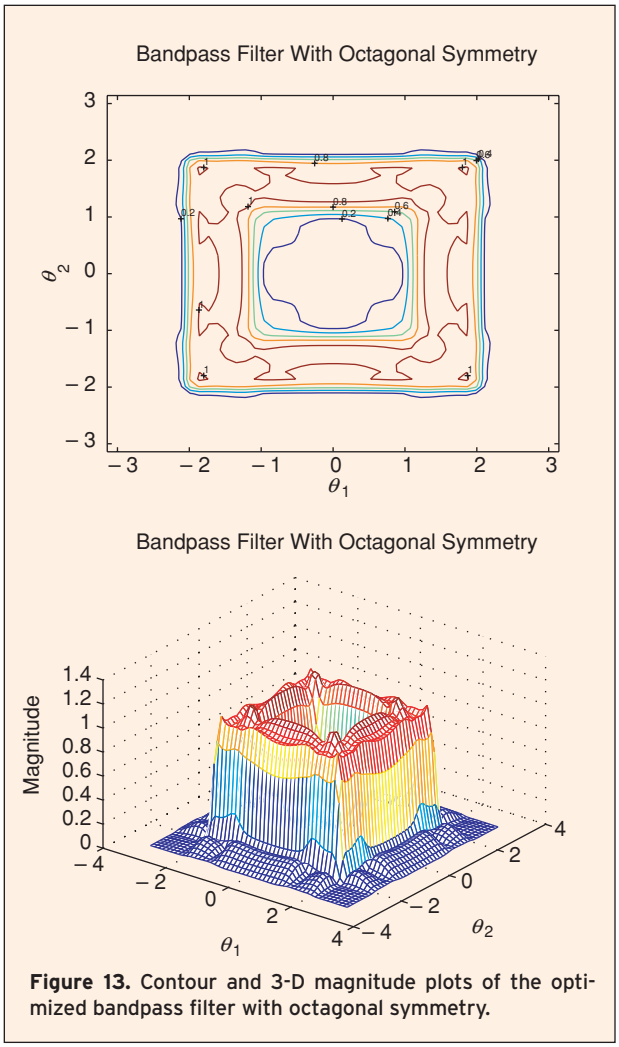

Figure 13. Contour and 3-D magnitude plots of the optimized bandpass filter with octagonal symmetry.

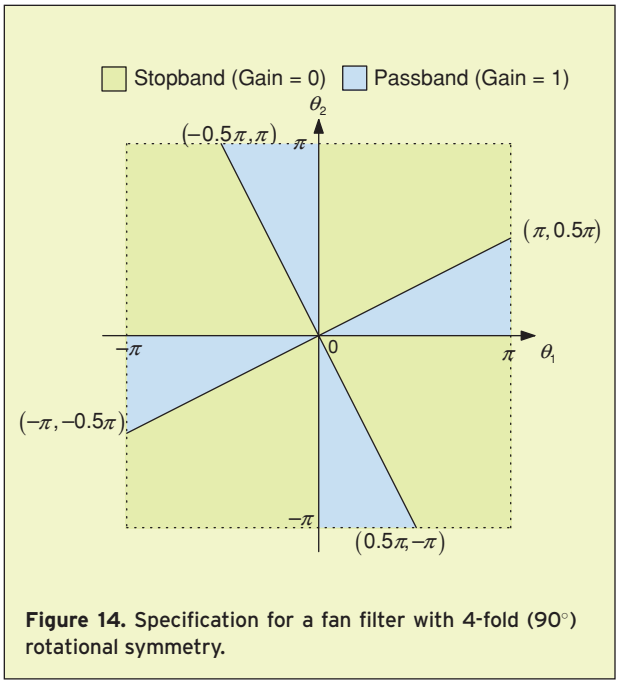

Figure 14. Specification for a fan filter with 4-fold (90°) rotational symmetry.

quency response induces a relation among the filter coefficients. This reduces the number of design parameters in an optimization scheme, as well as the number of multipliers in an implementation structure. Using the results discussed so far, we now present the optimization based design procedure for 2-D discrete-domain IIR filters with symmetry in the magnitude response.

Design Steps:

1. Identify the type of symmetry in the magnitude response specifications for the filter.
2. Assume a transfer function of the form:

$$H(z_1, z_2) = \frac{Q(z_1, z_2)}{D(z_1) \cdot D(z_2)} \qquad (44)$$

   Select the numerator from the list of polynomials in Table 6, such that it satisfies the required symmetry identified in Step 1. The denominator is chosen to be separable so that its stability can be easily assured. This denominator possesses octagonal symmetry and so satisfies quadrantal, diagonal, 4-fold rotational symmetries as well.
3. Select a suitable order for the filter such that the specifications can be met.
4. Choose a region in the (θ_1, θ_2) frequency plane to specify the desired magnitude response. For quadrantal, diagonal and rotational symmetries, the region need only be a 90° sector in the frequency plane. For octagonal symmetry, it need only be a 45° sector. Specify the frequency sample points in this region using concentric circles or rectangular grids.
5. Form an objective function to be minimized. This will be based on the difference between the magnitude response of the transfer function and the desired magnitude response, at the selected frequency points. One such objective function is:

$$J = \sum_k \sum_l [F(\theta_{1k}, \theta_{2l}) - F_d(\theta_{1k}, \theta_{2l})]^2 \qquad (45)$$

   where F is the magnitude squared response and θ_{1k}, θ_{2l} are the sample frequency points where the desired response is specified. In this function, the variables to be optimized are the coefficients of the transfer function.
6. Use any minimization algorithm, such as those provided in Matlab, to minimize the objective function J and obtain the optimal values for the filter coefficients. Verify that the filter specifications can be met with this set of filter coefficients. If not, make adjustment to the minimization algorithm and repeat the process.
7. Check the stability of the filter by finding the poles. Any unstable pole can be stabilized by replacing it with its inverse pole without affecting the magnitude response.

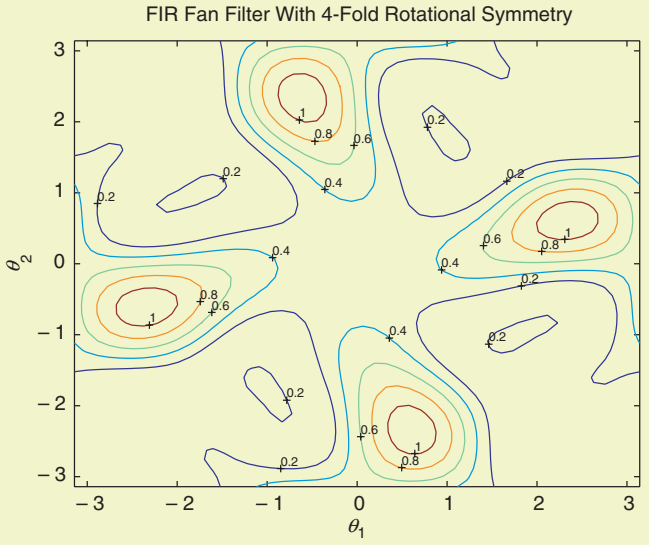

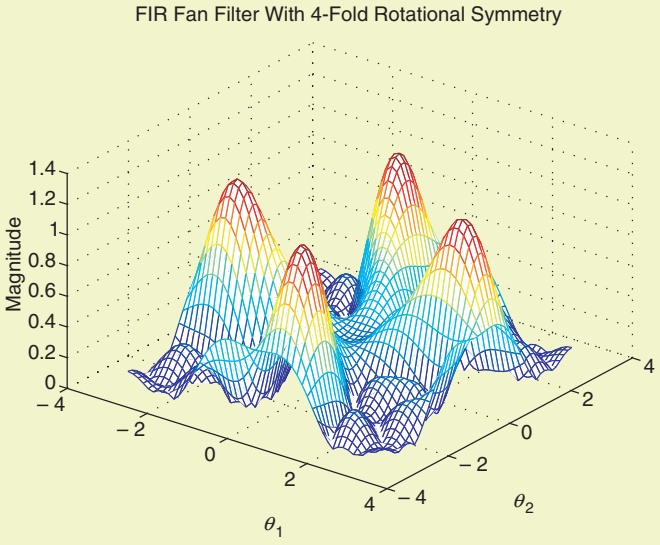

Figure 15. Contour and 3-D magnitude plots of the optimized FIR filter with 4-fold rotational symmetry.

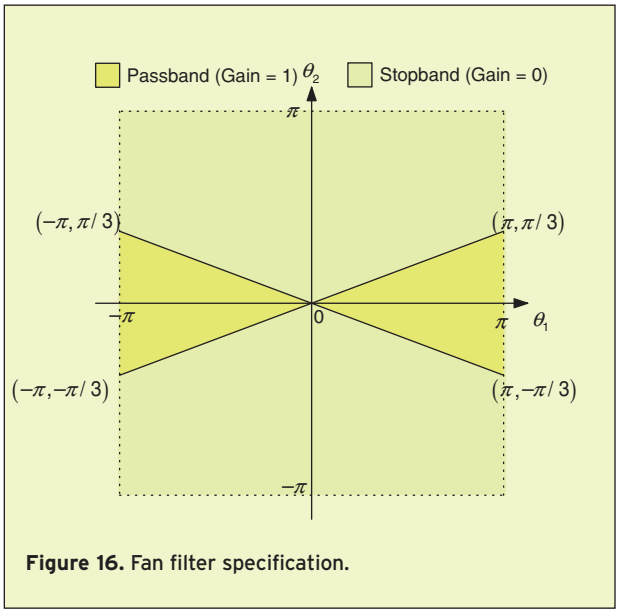

Figure 16. Fan filter specification.

Example 4: Using the procedure just discussed, we now design a bandpass filter with the filter specification shown in Figure 6.

It can be seen that the filter possesses diagonal symmetry. So we select the numerator to be $Q(z_1, z_2) = Q(z_2, z_1)$, which is Case (a) in the list of polynomials with diagonal symmetry in Table 6. We pick the order of the filter to be 4×4. The following are the forms for the numerator and denominator. It can be seen that the numerator coefficient matrix has diagonal symmetry. As a result, the number of variables to optimize is reduced from 50 (25 for the numerator and 25 for the denominator) to 19 (15 for the numerator and 4 for the denominator), a 62% reduction.

$$Q(z_1, z_2) = \begin{array}{c} \\ z_1^0 \\ z_1^1 \\ z_1^2 \\ z_1^3 \\ z_1^4 \end{array} \begin{array}{c} \begin{array}{ccccc} z_2^0 & z_2^1 & z_2^2 & z_2^3 & z_2^4 \end{array} \\ \begin{bmatrix} \boxed{a_{00}} & \boxed{a_{01}} & \boxed{a_{02}} & \boxed{a_{03}} & \boxed{a_{04}} \\ a_{01} & \boxed{a_{11}} & \boxed{a_{12}} & \boxed{a_{13}} & \boxed{a_{14}} \\ a_{02} & a_{12} & \boxed{a_{22}} & \boxed{a_{23}} & \boxed{a_{24}} \\ a_{03} & a_{13} & a_{23} & \boxed{a_{33}} & \boxed{a_{34}} \\ a_{04} & a_{14} & a_{24} & a_{34} & \boxed{a_{44}} \end{bmatrix} \end{array} \quad (46)$$

and

$$D(z_i) = b_0 + b_1 z_i + b_2 z_i^2 + b_3 z_i^3 + z_i^4 \ , \ i = 1, 2$$

We use the "lsqnonlin" routine in Matlab 5.3's Optimization Toolbox to minimize the objective function. Because of symmetry, we need only specify the desired response in a reduced region (90° sector) in the frequency plane. The transfer function coefficients of the optimized filter are listed on page 23, with the contour and 3-D magnitude plots given in Figure 7 on page 12. We verified that the filter is stable and meets the specification.

$a_{00} = 0.05691572886174$
$a_{01} = -0.02461862190217$
$a_{02} = 0.00986568924226$
$a_{03} = -0.01034804473379$
$a_{04} = 0.05820287661798$
$a_{11} = -0.02118017629239$
$a_{12} = -0.00404160157329$
$a_{13} = 0.03303916563349$
$a_{14} = -0.01033357674522$
$a_{22} = 0.00255022502754$
$a_{23} = -0.00398097317269$
$a_{24} = 0.00985123577827$
$a_{33} = -0.02118784417373$
$a_{34} = -0.02462035270181$
$a_{44} = 0.05691802180139$

$b_0 = 0.45583704915947$
$b_1 = -0.09763672454601$
$b_2 = 0.87533799314168$
$b_3 = -0.03923759607499$

Other types of filters can be designed using the same procedure. The following are some more examples.

Example 5: The filter specification in Figure 8 on page 13 possesses quadrantal symmetry. So we select the transfer function numerator to be $Q_1(z_1, z_2 + z_2^{-1}) \cdot Q_2(z_1 + z_1^{-1}, z_2)$. This is the product of Case (a) and (b) in the list of polynomials with quadrantal symmetry in Table 6. The filter order is chosen to be 4×4. The transfer function can be expressed as:

$$
\begin{aligned}
H(z) &= \frac{Q_1\left(z_1, z_2 + z_2^{-1}\right) \cdot Q_2\left(z_1 + z_1^{-1}, z_2\right)}{D(z_1) \cdot D(z_2)} \\
&= \frac{\left(\sum_{m=0}^{2}\sum_{n=0}^{1} a_{mn} \cdot z_1^m \cdot \left(z_2 + z_2^{-1}\right)^n\right) \cdot \left(\sum_{m=0}^{1}\sum_{n=0}^{2} b_{mn} \cdot \left(z_1 + z_1^{-1}\right)^m \cdot z_2^n\right)}{\left(z_1^4 + \sum_{i=0}^{3} d_i z_1^i\right) \cdot \left(z_2^4 + \sum_{i=0}^{3} d_i z_2^i\right)}
\end{aligned}
$$

The following are the optimized filter coefficients. Because of the quadrantal symmetry constraints, the number of independent variables to optimize is reduced from 50 to 16 (12 for the numerator and 4 for the denominator), a 68% reduction. The resulting contour and 3-D plots are shown in Figure 9 on page 13.

$a_{00} = -0.36223343641959$
$a_{10} = 0.73781886914067$
$a_{20} = -0.35115585228984$
$a_{01} = 0.18001689678736$
$a_{11} = -0.23263738256684$
$a_{21} = 0.18813447360982$

$b_{00} = 0.49109027165487$
$b_{01} = 0.31981445338169$
$b_{02} = 0.49120885907429$
$b_{10} = -0.11409694648059$
$b_{11} = -0.38504269416613$
$b_{12} = -0.11398910827760$

$d_0 = -0.02550110734351$
$d_1 = -0.01599046367101$
$d_2 = 0.37661874629072$
$d_3 = -1.06746935205100$

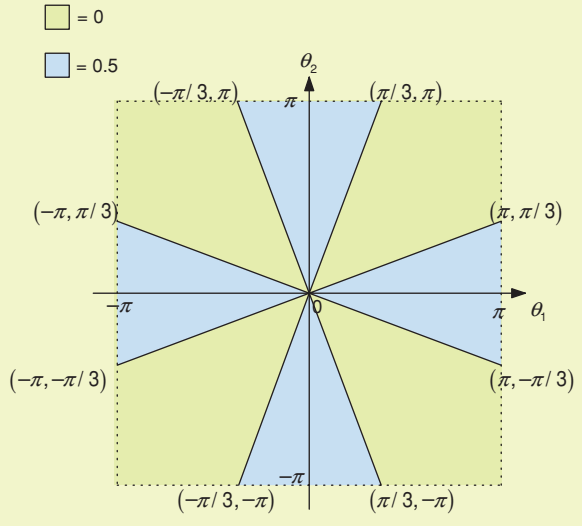

Figure 17. Octagonally symmetrical component of response.

Example 6: It can be observed that the filter specification in Figure 10 on page 20 possesses 4-fold (90°) rotational symmetry. So, we select the transfer function numerator to be $Q(z_1, z_2) \cdot Q(z_2, z_1^{-1})$, which is Case (d) for polynomials with 4-fold rotational symmetry in Table 6. The filter order is chosen to be 5×5 and the transfer function can be written as:

$$H(z) = \frac{Q(z_1, z_2) \cdot Q\left(z_2, z_1^{-1}\right)}{D(z_1) \cdot D(z_2)} = \frac{\left(\sum_{m=0}^{4}\sum_{n=0}^{1} a_{mn} z_1^m z_2^n\right) \cdot \left(\sum_{m=0}^{4}\sum_{n=0}^{1} a_{mn} z_2^m z_1^{-n}\right)}{\left(z_1^5 + \sum_{i=0}^{4} d_i z_1^i\right) \cdot \left(z_2^5 + \sum_{i=0}^{4} d_i z_2^i\right)}$$

The following are the optimized filter coefficients. Here, the number of independent variables to optimize is reduced from 72 to 15 (10 for the numerator and 5 for the denominator), a 79% reduction. The resulting contour and 3-D perspective plots are shown in Figure 11 on page 20.

$$\begin{aligned}
a_{00} &= 0.20294324476412 \\
a_{01} &= -0.48163632801449 \\
a_{10} &= 0.36932528231741 \\
a_{11} &= 0.18286723039587 \\
a_{20} &= -0.60107454130023 \\
a_{21} &= 0.57969763481886 \\
a_{30} &= -0.08314333950507 \\
a_{31} &= -0.32680233587436 \\
a_{40} &= 0.12928331110133 \\
a_{41} &= -0.02087010625653
\end{aligned}$$

$$\begin{aligned}
d_0 &= 0.03480848557051 \\
d_1 &= -0.34376565481538 \\
d_2 &= 0.76070962863907 \\
d_3 &= -0.08613899671423 \\
d_4 &= -1.31455055755094
\end{aligned}$$

Example 7: In this example, we are required to design a filter to meet the specifications given in Figure 12 on page 20.

It can be seen that the response possesses octagonal symmetry. So using Table 6 and assuming the filter order to be 6×6, we can write the transfer function as:

$$H(z) = \frac{Q\left(z_1 + z_1^{-1}, z_2\right) \cdot Q\left(z_2 + z_2^{-1}, z_1\right)}{D(z_1) \cdot D(z_2)} = \frac{\left(\sum_{m=0}^{1}\sum_{n=0}^{4} a_{mn} \cdot \left(z_1 + z_1^{-1}\right)^m \cdot z_2^n\right) \cdot \left(\sum_{m=0}^{1}\sum_{n=0}^{4} a_{mn} \cdot \left(z_2 + z_2^{-1}\right)^m \cdot z_1^n\right)}{\left(z_1^6 + \sum_{i=0}^{5} d_i z_1^i\right) \cdot \left(z_2^6 + \sum_{i=0}^{5} d_i z_2^i\right)}$$

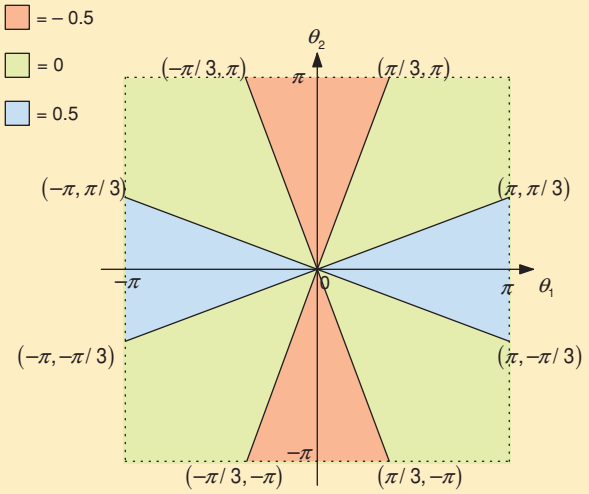

Figure 18. Octagonally antisymmetrical component of response.

The transfer function numerator chosen is Case (b) in the list of polynomials with octagonal symmetry.

Here, the advantage of employing the symmetry constraints is that the number of independent coefficients to optimize is reduced from 98 to 16 (10 for the numerator and 6 for the denominator), an 84% reduction. Also, because of octagonal symmetry, the optimization need only be done in a reduced 45° degree sector in the frequency plane, which gives further reduction in computational time. The optimized filter coefficients are shown below. The contour and 3-D plots of the optimized filter are shown in Figure 13 on page 21.

$$\begin{aligned}
a_{00} &= -0.02676667082778 \\
a_{01} &= -0.30824801305310 \\
a_{02} &= -0.61338664353594 \\
a_{03} &= -0.54784348150223 \\
a_{04} &= -0.23052991083493
\end{aligned}$$

$$\begin{aligned}
a_{10} &= -0.08712047342727 \\
a_{11} &= 0.10230094916767 \\
a_{12} &= 0.44881705473037 \\
a_{13} &= 0.53311155984782 \\
a_{14} &= 0.28348672960777
\end{aligned}$$

$$\begin{aligned}
d_0 &= 0.07858008457571 \\
d_1 &= -0.10704620692704 \\
d_2 &= 0.66811506285393 \\
d_3 &= -0.19413076009780 \\
d_4 &= 1.15029323700482 \\
d_5 &= -0.09513351068716
\end{aligned}$$

Table 7.
Polynomial factors possessing symmetry and stability.

Continuous domain	Discrete domain
Quadrantal Symmetry $D(s_1, s_2) = D_1(s_1) \cdot D_2(s_2)$ where D_1 and D_2 are stable 1-D polynomials.	Quadrantal Symmetry $D(z_1, z_2) = D_1(z_1) \cdot D_2(z_2)$ where D_1 and D_2 are stable 1-D polynomials.
Diagonal Symmetry $D(s_1, s_2) = D(s_2, s_1)$ where D is stable.	Diagonal Symmetry $D(z_1, z_2) = D(z_2, z_1)$ where D is stable.
Four-Fold (90°) Rotational Symmetry $D(s_1, s_2) = D_1(s_1) \cdot D_1(s_2)$ where D_1 is a stable 1-D polynomial.	Four-Fold (90°) Rotational Symmetry $D(z_1, z_2) = D_1(z_1) \cdot D_1(z_2)$ where D_1 is a stable 1-D polynomial.
Octagonal Symmetry $D(s_1, s_2) = D_1(s_1) \cdot D_1(s_2)$ where D_1 is a stable 1-D polynomial.	Octagonal Symmetry $D(z_1, z_2) = D_1(z_1) \cdot D_1(z_2)$ where D_1 is a stable 1-D polynomial.

FIR Filter Design

Just like for IIR filters, symmetry can also be used to reduce the complexity in the design of 2-D finite impulse response (FIR) filters. The transfer function of a 2-D FIR filter has the form $\sum_m \sum_n h_{mn} \cdot z_1^m \cdot z_2^n$, where the coefficients h_{mn} are the impulse response samples. An FIR filter can be designed to possess linear phase which makes it attractive in certain applications. However, the disadvantage is that it often requires a much higher filter order to satisfy the same specification compared to an IIR filter.

In the following, we present an FIR design example utilizing symmetry. We use basically the same design steps presented previously for IIR filters, except that step 7 is not needed here since an FIR filter is always stable.

Example 8: The filter specification shown in Figure 14 on page 21 possesses 4-fold (90°) rotational symmetry. So, using Table 6, we write the filter transfer function as:

$$H(z_1, z_2) = \{Q_1(x_1, x_2) + y_1 y_2 \cdot (x_1 - x_2) \cdot Q_2(x_1, x_2)\} \cdot z_1^{\alpha} \cdot z_2^{\alpha} \quad (47)$$

where $Q_k(x_1, x_2) = Q_k(x_2, x_1)$ for $k = 1, 2$.

This is Case (a) in the polynomials with rotational symmetry. (The z_1^{α} and z_2^{α} factors are included to ensure the polynomial nature of $H(z_1, z_2)$). The polynomial in (47) is the result of the symmetry condition $H(z_1, z_2) = H(z_2^{-1}, z_1) \cdot z_2^N$. Consequently, the coefficients have to satisfy the condition $h_{mn} = h_{n,N-m}$, which

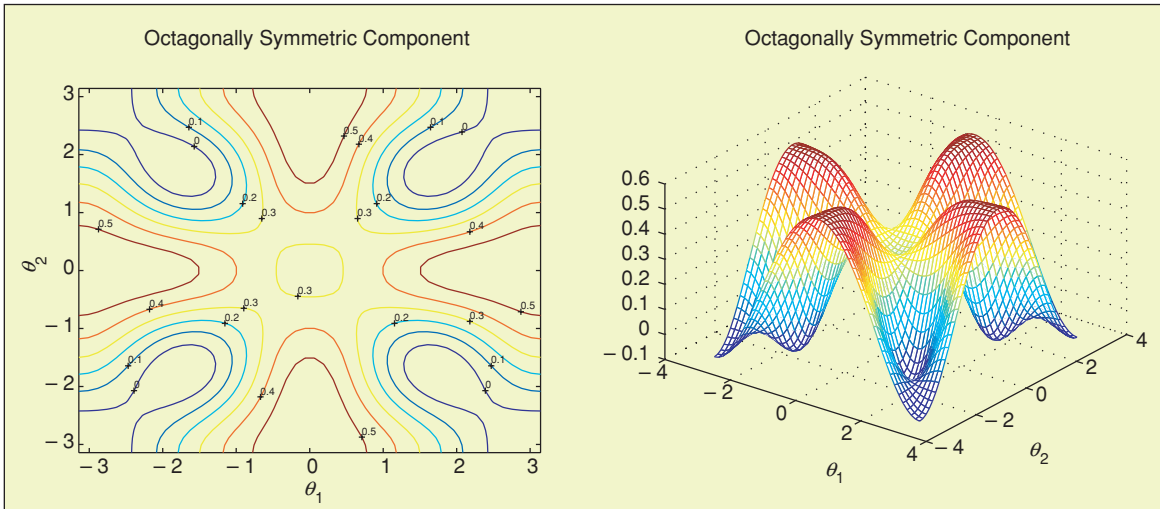

Figure 19. Contour and 3-D plots of the symmetric component.

Table 8.
Coefficient conditions for various symmetries on polynomial $P(\theta)$ in (52).

Name of Symmetry	Condition on Symmetry	Condition on Antisymmetry
Quadrantal	$b_{mn} = 0$	$a_{kl} = 0$
Diagonal $b_{mn} = b_{nm}$	$a_{kl} = a_{lk}$ $b_{mn} = -b_{nm}$	$a_{kl} = -a_{lk}$
Four-Fold (90°) rotational $b_{mn} = -b_{nm}$	$a_{kl} = a_{lk}$ $b_{mn} = b_{nm}$	$a_{kl} = -a_{lk}$
Octagonal	$a_{kl} = a_{lk}$ $b_{mn} = 0$	i) $a_{kl} = 0, b_{mn} = b_{nm}$ ii) $a_{kl} = -a_{lk}, b_{mn} = 0$ iii) $a_{kl} = 0, b_{mn} = -b_{nm}$

means that the coefficient matrix has to possess 4-fold (90°) rotational symmetry. The coefficient matrix is shown below for a filter of impulse response (coefficient) size of 7×7. It can be seen that only the boxed coefficients are independent, and the other coefficients can be obtained by rotating the boxed coefficients in steps of 90° around the mid-point of the whole matrix.

$$H(z_1, z_2) = \begin{array}{c} \\ z_1^0 \\ z_1^1 \\ z_1^2 \\ z_1^3 \\ z_1^4 \\ z_1^5 \\ z_1^6 \end{array} \begin{array}{c} \begin{array}{ccccccc} z_2^0 & z_2^1 & z_2^2 & z_2^3 & z_2^4 & z_2^5 & z_2^6 \end{array} \\ \begin{bmatrix} \boxed{a_{00}} & \boxed{a_{01}} & \boxed{a_{02}} & \boxed{a_{03}} & a_{20} & a_{10} & a_{00} \\ \boxed{a_{10}} & \boxed{a_{11}} & \boxed{a_{12}} & \boxed{a_{13}} & a_{21} & a_{11} & a_{01} \\ \boxed{a_{20}} & \boxed{a_{21}} & \boxed{a_{22}} & \boxed{a_{23}} & a_{22} & a_{12} & a_{02} \\ a_{03} & a_{13} & a_{23} & \boxed{a_{33}} & a_{23} & a_{13} & a_{03} \\ a_{02} & a_{12} & a_{22} & a_{23} & a_{22} & a_{21} & a_{20} \\ a_{01} & a_{11} & a_{21} & a_{13} & a_{12} & a_{11} & a_{10} \\ a_{00} & a_{10} & a_{20} & a_{03} & a_{02} & a_{01} & a_{00} \end{bmatrix} \end{array}$$

Because of the symmetry constraint, the number of independent coefficients is 13, a 73% reduction from the original 49. The optimized filter coefficients are shown below and the resulting filter response is shown in Figure 15 on page 22.

$$a_{00} = -6.2016 \times 10^{-3}$$
$$a_{01} = -52.534 \times 10^{-3}$$
$$a_{02} = 45.586 \times 10^{-3}$$
$$a_{03} = 7.3391 \times 10^{-3}$$
$$a_{10} = 23.106 \times 10^{-3}$$
$$a_{11} = -32.25 \times 10^{-3}$$
$$a_{12} = 66.891 \times 10^{-3}$$
$$a_{13} = 52.406 \times 10^{-3}$$
$$a_{20} = -13.519 \times 10^{-3}$$
$$a_{21} = -78.678 \times 10^{-3}$$
$$a_{22} = -68.031 \times 10^{-3}$$
$$a_{23} = 49.386 \times 10^{-3}$$
$$a_{33} = 0.23983$$

It is to be noted that the choice of transfer function here results in a filter with linear phase. This is because on substituting $z_i = e^{-j\theta_i}$ into the transfer function, we get

$$H(\theta_1, \theta_2) = \{Q_1(\cos\theta_1, \cos\theta_2) + \sin\theta_1 \cdot \sin\theta_2 \times (\cos\theta_1 - \cos\theta_2) \cdot Q_2(\cos\theta_1, \cos\theta_2)\} \times e^{-j\alpha\cdot\theta_1} \cdot e^{-j\alpha\cdot\theta_2}$$

The expression $\{Q_1(\cos\theta_1, \cos\theta_2) + \sin\theta_1 \cdot \sin\theta_2 \cdot (\cos\theta_1 - \cos\theta_2) \cdot Q_2(\cos\theta_1, \cos\theta_2)\}$ is real. Thus, $\angle H(\theta_1, \theta_2) = -\alpha \cdot (\theta_1 + \theta_2) + k \cdot \pi$, where k is an integer, and so the phase is linear.

Symmetrical Decomposition and Transformation

Among the methods used in the design of 2-D FIR filters, optimization, window techniques, and transformation are the most popular. In this section, we first present techniques to improve the efficiency and versatility of the transformation method by making use of the symmetry properties of the transformation functions. After that, we describe a procedure to extend the application of symmetry properties to the design of filters that do not possess identifiable symmetry in their frequency responses. The approach that is followed is to decompose the given specification into a number of components each possessing some form of symmetry.

1-D to 2-D Transformation

Among the various methods available for the design of 2-D FIR filters, transformation method has been found to be the simplest and most efficient one for many specifications. Introduced by McClellan in 1973, this method has been studied extensively by a number of research workers in this field. Here, we present techniques to improve the efficiency and versatility of this method by making use of the symmetry properties of transformation functions.

Let $G(u)$ represent the frequency response of a 1-D FIR filter. Then $G(u)$ can be written as

$$G(u) = g(0) + \sum_{n=1}^{N} 2 \cdot g(n) \cdot \cos(nu) \qquad (48)$$

where $g(n)$ is the impulse response sequence of the 1-D FIR filter. Expressing $\cos(nu)$ in terms of $\cos(u)$, we can rewrite (48) as

$$G(u) = \sum_{n=0}^{N} b_n \cdot (\cos u)^n = \hat{G}(\cos u) \tag{49}$$

The generalized McClellan transformation which converts the 1-D zero phase FIR filter into a 2-D zero phase FIR filter is given by

$$\cos u = P(\underline{\theta}) = P(\cos\theta_1, \cos\theta_2, \sin\theta_1, \sin\theta_2) \tag{50}$$

where $P(\underline{\theta})$ can be considered as the frequency response function of a 2-D zero phase FIR filter. Substitution of (50) in (49) gives a 2-D zero phase frequency response function as

$$H(\underline{\theta}) = \hat{G}(P(\underline{\theta})) = \hat{H}(\cos\theta_1, \cos\theta_2, \sin\theta_1, \sin\theta_2) \tag{51}$$

It may be easily verified that the response of $H(\underline{\theta})$ at a point $\underline{\theta}_i$ is given by $G(\cos^{-1}[P(\underline{\theta}_i)])$, i.e., the response of $G(u)$ at $u = \cos^{-1}[P(\underline{\theta}_i)]$. This means that all those points in the (θ_1, θ_2) plane where $P(\underline{\theta}) = P(\underline{\theta}_i)$, the response will have a constant value and the line joining these points will constitute a constant value contour. In other words, the response of the 1-D function $G(u)$ is carried over to the 2-D plane by the transformation (50). The actual response values of these contours are determined by $G(u)$. Very often, the specified 2-D response possesses some form of symmetry in addition to being real, and the utilization of this symmetry will reduce the complexity of the filter design.

Symmetry constraints on transformation functions

From the previous discussion on the generation of 2-D functions using transformation functions, it should be apparent that the symmetry properties of the generated 2-D function will depend on the symmetry properties of the 1-D base function $G(u)$ and the 2-D transformation function $P(\underline{\theta})$. We will now investigate the natures of $G(u)$ and $P(\underline{\theta})$ such that the generated function $H(\underline{\theta})$ possesses a desired T-symmetry or T-antisymmetry. In this context, we state a number of theorems that outline these properties.

Theorem 7: If $P(\underline{\theta})$ possesses a T-symmetry, then $H(\underline{\theta}) = \hat{G}(P(\underline{\theta}))$ possesses the same T-symmetry independent of the nature of $G(u)$.

Theorem 8: If $P(\underline{\theta})$ possesses a T-antisymmetry and $G(u) = G(\pi - u)$, i.e., $G(u)$ possesses a reflection symmetry about $u = \pi/2$, then $H(\underline{\theta}) = \hat{G}(P(\underline{\theta}))$ possesses the T-symmetry. It is to be noted that $G(u) = G(\pi - u)$ if it can be expressed as $G(u) = \sum_{n=0}^{N} c_n(\cos u)^{2n}$.

Theorem 9: If $P(\underline{\theta})$ possesses a T-antisymmetry and $G(u) = -G(\pi - u)$, i.e., $G(u)$ possesses a reflection antisymmetry about $u = \pi/2$, then $H(\underline{\theta}) = \hat{G}(P(\underline{\theta}))$ possesses the T-antisymmetry. It is to be noted that $G(u) = -G(\pi - u)$ if it can be written as $G(u) = \sum_{n=0}^{N} c_n(\cos u)^{2n+1}$.

The above three theorems give sufficient conditions for $H(\underline{\theta})$ to possess T-symmetry or T-antisymmetry. Therefore, based on the symmetry of the desired response, one can choose suitable forms of $P(\underline{\theta})$ and $G(u)$. The following is an example to illustrate the application of Theorem 8.

Example 9: Let $G(u) = 1 - 2 \cdot (\cos u)^2$ and $P(\underline{\theta}) = 0.5\cos\theta_1 - 0.5\cos\theta_2$. Then

$$\begin{aligned} H(\underline{\theta}) &= 1 - 2 \cdot (0.5\cos\theta_1 - 0.5\cos\theta_2)^2 \\ &= 1 - 0.5\cos^2\theta_1 - 0.5\cos^2\theta_2 + \cos\theta_1\cos\theta_2 \end{aligned}$$

It is verified that $G(u) = G(\pi - u)$ and $P(\underline{\theta})$ possesses $x_1 = x_2$ diagonal reflection antisymmetry and as expected $H(\underline{\theta})$ possesses $x_1 = x_2$ diagonal reflection symmetry.

We next consider the constraints on $P(\underline{\theta})$ explicitly for some types of T-symmetries and antisymmetries. We note that the zero phase transformation function $P(\underline{\theta})$ can be written as:

$$\begin{aligned} P(\underline{\theta}) = &\sum_{k=0}^{K}\sum_{l=0}^{L} a_{kl} \cdot (\cos\theta_1)^k \cdot (\cos\theta_2)^l \\ &+ \sin\theta_1 \cdot \sin\theta_2 \cdot \sum_{m=0}^{M}\sum_{n=0}^{N} b_{mn} \cdot (\cos\theta_1)^m \cdot (\cos\theta_2)^n \end{aligned} \tag{52}$$

Different types of symmetries and antisymmetries impose constraints on the coefficients a_{kl} and b_{mn}. These constraints are listed in Table 8 on page 26.

It often happens that a desired specification possesses more than one form of symmetry. In this case, applying Theorems 7 to 9, one can develop the properties of $P(\underline{\theta})$ and $G(u)$ such that the generated function $H(\underline{\theta})$ possesses the required symmetries. Along these lines, the following two theorems present useful results.

Theorem 10: For a transformed function $H(\underline{\theta})$ to possess T_k-identity, $k = 1, \ldots, n$, symmetries, either of the following choices may be made

(i) $P(\underline{\theta})$ possesses $T_1, T_2, \ldots, T_n$ identity symmetries and no constraint is placed on $G(u)$.

or

(ii) $G(u) = G(\pi - u)$ and $P(\underline{\theta})$ possesses $T_1, T_2, \ldots, T_n$ identity or antisymmetries, i.e., each T_k symmetry can be either identity or antisymmetry.

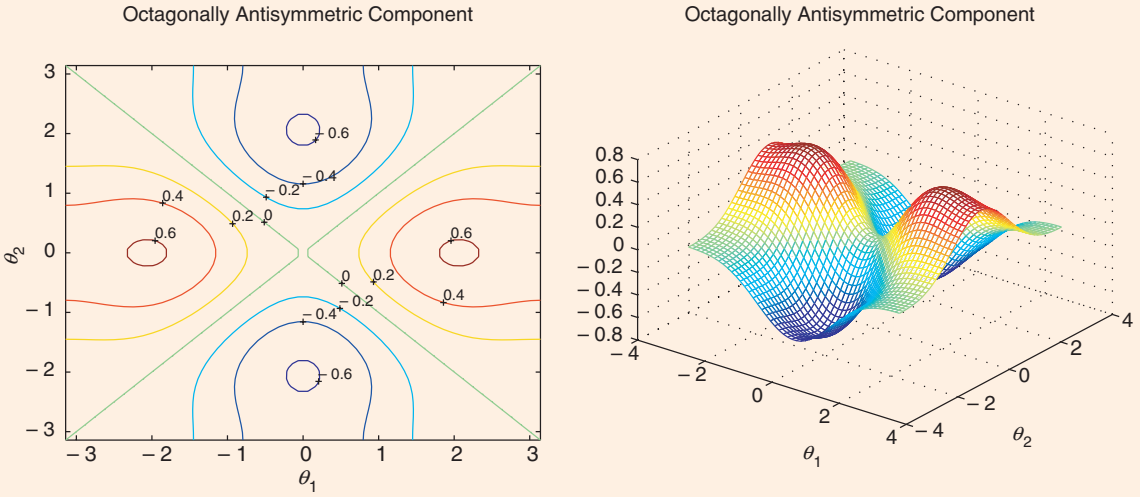

Figure 20. Contour and 3-D plots of the antisymmetric component.

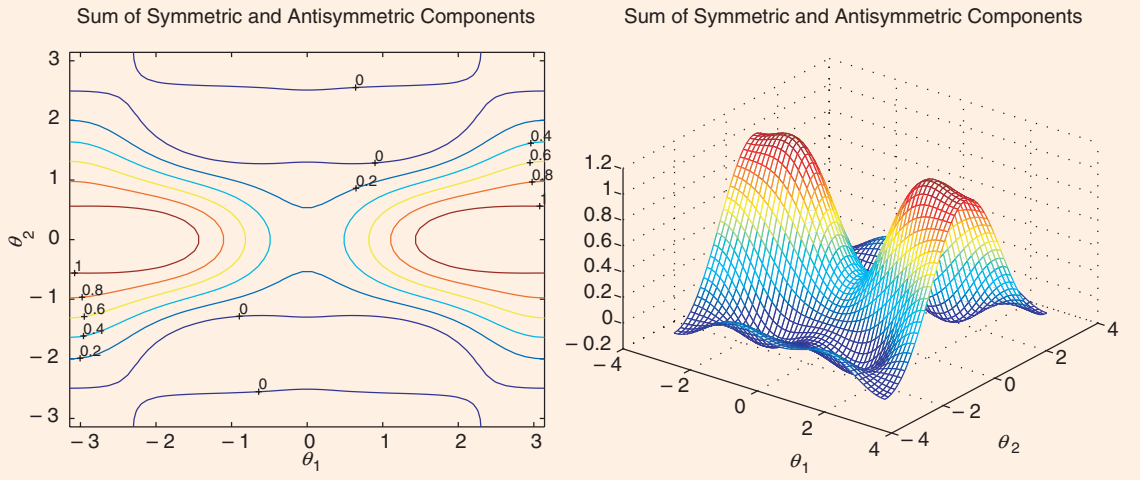

Figure 21. Contour and 3-D plots of the total response.

Theorem 11: For a transformed function $H(\underline{\theta})$ to possess T_k-identity/ anti- symmetry, $k = 1, \ldots, n$, (some or all of them can be antisymmetries), the following choice will meet the requirement: $P(\underline{\theta})$ possesses the designated T_k-identity/antisymmetries of $H(\underline{\theta})$ for $k = 1, \ldots, n$, and $G(u) = -G(\pi - u)$.

Application of the symmetry constraints

The different constraints established for the base and transformation functions will find their application in the proper choice of $G(u)$ and $P(\underline{\theta})$. This proper choice in turn will lead to a reduction in the number of unknowns to be determined by the design methods such as optimization. In this connection, Table 8 will help one to choose a proper $P(\underline{\theta})$. For example, if 4-fold rotational symmetry is desired for $P(\underline{\theta})$, we have from Table 8, $a_{kl} = a_{lk}$ and $b_{mn} = -b_{nm}$. In the lowest order case, we can write $P(\underline{\theta})$ as

$$P(\underline{\theta}) = a + b \cdot (\cos\theta_1 + \cos\theta_2) + c \cdot \cos\theta_1 \cdot \cos\theta_2 + d \cdot \sin\theta_1 \cdot \sin\theta_2 \cdot (\cos\theta_1 - \cos\theta_2)$$

where a, b, c, and d are to be determined to give the necessary contour shapes. This choice thus results in a reduction of the number of unknowns from 8 to 4.

Symmetrical Decomposition

If the specified 2-D response does not possess any easily identifiable symmetry, then the above properties cannot be made use of. A solution to this problem is to decompose the given specification into a number of components each having some form of symmetry [27, 28]. As the complexity of the design of the components

with symmetry is lower than that of the original specification, the design based on symmetric decomposition is more efficient than the conventional design. The design procedure then consists of the following three steps.

1. The given 2-D specification is decomposed into a number of symmetrical components such as quadrantal symmetric and antisymmetric components, diagonal symmetric and antisymmetric components, etc.
2. Each symmetrical component is designed separately using a design procedure such that the symmetry properties are used effectively.
3. The designed filters corresponding to the different components are combined either in the transfer function level or in the implementation level to obtain the total filter.

We will next consider the steps 1 and 2 in more detail.

Decomposition technique

To utilize the symmetry properties discussed, a function $f(\underline{x})$ needs to have a symmetry or an antisymmetry with respect to an operation T. When $f(\underline{x})$ does not meet this requirement, we can still employ symmetry properties in their design if we are able to decompose $f(\underline{x})$ into T-symmetric and T-antisymmetric components. We will next consider under what conditions such a decomposition exists and how a given $f(\underline{x})$ can be decomposed.

Let us assume that with respect to a symmetry operation T, $f(\underline{x})$ is decomposable as

$$f(\underline{x}) = f_+(\underline{x}) + f_-(\underline{x}) \tag{53}$$

where

$$f_+(\underline{x}) = f_+(T[\underline{x}]), \text{ (symmetric component)} \tag{54}$$

and

$$f_-(\underline{x}) = -f_-(T[\underline{x}]), \text{ (antisymmetric component)} \tag{55}$$

then

$$f(T[\underline{x}]) = f_+(T[\underline{x}]) + f_-(T[\underline{x}]) = f_+(\underline{x}) - f_-(\underline{x}) \tag{56}$$

Now from (53) and (56) we can find $f_+(\underline{x})$ and $f_-(\underline{x})$ as

$$f_+(\underline{x}) = \tfrac{1}{2} \cdot \{f(\underline{x}) + f(T[\underline{x}])\}$$

and

$$f_-(\underline{x}) = \tfrac{1}{2} \cdot \{f(\underline{x}) - f(T[\underline{x}])\}$$

Now to verify that such a decomposition is possible, $f_+(\underline{x})$ and $f_-(\underline{x})$ should satisfy (54) and (55), i.e.,

$$\begin{aligned} f_+(T[\underline{x}]) &= \tfrac{1}{2} \cdot \{f(T[\underline{x}]) + f(T[T[\underline{x}]])\} \\ &= \tfrac{1}{2} \cdot \{f(T[\underline{x}]) + f(T^2[\underline{x}])\} \end{aligned}$$

As $f_+(\underline{x}) = f_+(T[\underline{x}])$,

$$\begin{aligned} \tfrac{1}{2} \cdot \{f(\underline{x}) + f(T[\underline{x}])\} = \tfrac{1}{2} \cdot \{f(T[\underline{x}]) + f(T^2[\underline{x}])\}, \\ \text{i.e.,} f(\underline{x}) = f(T^2[\underline{x}]) \end{aligned} \tag{57}$$

Similarly substituting

$$f_-(T[\underline{x}]) = \tfrac{1}{2} \cdot \{f(T[\underline{x}]) - f(T^2[\underline{x}])\}$$

in (55) we get

$$\begin{aligned} \tfrac{1}{2} \cdot \{f(\underline{x}) - f(T[\underline{x}])\} &= \tfrac{1}{2} \cdot \{f(T^2[\underline{x}]) - f(T[\underline{x}])\} \\ \text{i.e., } f(\underline{x}) &= f(T^2[\underline{x}]) \end{aligned} \tag{58}$$

The conditions (57) and (58) may be satisfied if and only if either i) T^2 is an identity operation or ii) $f(\underline{x})$ has T^2-identity symmetry. This can be stated in the form of a theorem.

Theorem 12: With respect to a symmetry operation T, $f(\underline{x})$ can be decomposed into two components as

$$f(\underline{x}) = f_+(\underline{x}) + f_-(\underline{x})$$

where $f_+(\underline{x})$ possesses T-identity symmetry and $f_-(\underline{x})$ possesses T-antisymmetry if and only if either T is a 2-cyclic operation or $f(\underline{x})$ possesses T^2-identity symmetry. Then the components are given by

$$\begin{bmatrix} f_+(\underline{x}) \\ f_-(\underline{x}) \end{bmatrix} = \frac{1}{2} \begin{bmatrix} 1 & 1 \\ 1 & -1 \end{bmatrix} \begin{bmatrix} f(\underline{x}) \\ f(T[\underline{x}]) \end{bmatrix}$$

The following are examples to illustrate this.

Example 10: Let $f(\underline{x}) = 1 + 2x_1 + 3x_2 + 4x_1x_2$ and $T = T_1 = \begin{bmatrix} 1 & 0 \\ 0 & -1 \end{bmatrix}$. From "Nature of T-Operations," we know that T_1 represents reflection about the x_1-axis, a 2-cyclic operation. So using Theorem 12, we can decompose $f(\underline{x})$ into $f_+(\underline{x}) = 1 + 2x_1$ and $f_-(\underline{x}) = 3x_2 + 4x_1x_2$, where $f_+(\underline{x})$ and $f_-(\underline{x})$ possess T_1-identity symmetry and T_1 antisymmetry respectively.

Example 11: Let $f(\underline{x}) = 1 + 2x_1x_2 + 3x_1^2 + 4x_2^2$ and $T = T_6 = \begin{bmatrix} 0 & -1 \\ 1 & 0 \end{bmatrix}$. T_6 represents 90° anti-clockwise rotation about the origin, which is a 4-cyclic operation and not 2-cyclic. So, in order to apply Theorem 12, $f(\underline{x})$ needs to possess T_6^2-identity symmetry. It is easy to verify

that $f(T_6^2[\underline{x}]) = f(-\underline{x}) = \quad 1 + 2x_1x_2 + 3x_1^2 + 4x_2^2 = f(\underline{x})$, hence decomposition is possible. Using Theorem 12, we get $f_+(\underline{x}) = \quad 1 + 3.5x_1^2 + 3.5x_2^2$ and $f_-(\underline{x}) = 2x_1x_2 - 0.5x_1^2 + 0.5x_2^2$, where $f_+(\underline{x})$ and $f_-(\underline{x})$ possess T_6-identity symmetry and T_6 antisymmetry respectively.

Extending the above technique, one can decompose $f(\underline{x})$ into four components such that each component possesses symmetry or antisymmetry with respect to two symmetry operations. This is explained in the next theorem.

Theorem 13: $f(\underline{x})$ can be decomposed into four components as

$$f(\underline{x}) = f_{++}(\underline{x}) + f_{+-}(\underline{x}) + f_{-+}(\underline{x}) + f_{--}(\underline{x})$$

where

$f_{++}(\underline{x})$ possesses T_a-symmetry and T_b-symmetry
$f_{+-}(\underline{x})$ possesses T_a-symmetry and T_b-antisymmetry
$f_{-+}(\underline{x})$ possesses T_a-antisymmetry and T_b-symmetry
$f_{--}(\underline{x})$ possesses T_a-antisymmetry and T_b-antisymmetry

if T_a and T_b are 2-cyclic and $T_aT_b = T_bT_a$. The components are then given by

$$\begin{bmatrix} f_{++}(\underline{x}) \\ f_{+-}(\underline{x}) \\ f_{-+}(\underline{x}) \\ f_{--}(\underline{x}) \end{bmatrix} = \frac{1}{4} \begin{bmatrix} 1 & 1 & 1 & 1 \\ 1 & 1 & -1 & -1 \\ 1 & -1 & 1 & -1 \\ 1 & -1 & -1 & 1 \end{bmatrix} \cdot \begin{bmatrix} f(\underline{x}) \\ f(T_a[\underline{x}]) \\ f(T_b[\underline{x}]) \\ f(T_a[T_b[\underline{x}]]) \end{bmatrix}$$

The following example illustrates the application of the above theorem.

Example 12: Let $f(\underline{x}) = 1 + 2x_1 + 3x_2 + 4x_1x_2$, $T_a = T_3 = \begin{bmatrix} 0 & 1 \\ 1 & 0 \end{bmatrix}$, and $T_b = T_4 = \begin{bmatrix} 0 & -1 \\ -1 & 0 \end{bmatrix}$. From "The Nature of T-Operations," we know that T_a is reflection about $x_1 = x_2$ diagonal, and T_b is reflection about $x_1 = -x_2$ diagonal, both of which are 2-cyclic operations. Also $T_aT_b = T_bT_a$. So we can use Theorem 13 to obtain:

$$\begin{aligned} f_{++}(\underline{x}) &= 1 + 4x_1x_2 \\ f_{+-}(\underline{x}) &= 2.5x_2 + 2.5x_1 \\ f_{-+}(\underline{x}) &= 0.5x_2 - 0.5x_1 \\ f_{--}(\underline{x}) &= 0 \end{aligned}$$

One can extend the above technique to decompose a given response into eight or larger number of components if the symmetry operations satisfy certain conditions.

In the following we will consider the application of decomposition to 2-D filter design.

FIR Filter Design Based on Decomposition

In the design of filters using decomposition, the given frequency response specification is decomposed into a number of symmetrical and antisymmetrical components. Each component can then be designed using any of the general approximation methods. Here, we employ the optimization based procedure for this purpose. It is expected that symmetrical decomposition will result in a substantial reduction in the complexity in the optimization based procedure for the following reasons:

(i) The complexity of an optimization scheme is generally proportional to the square of the number of parameters to be optimized.
(ii) The number of parameters to be optimized for each component is much smaller than that for the whole filter and the total number of parameters of all the components together for a given order filter is no more than that for the undecomposed scheme.

It is to be noted that even if the original filter specification possesses symmetry, decomposition can still be applied and this will also result in reduction in the complexity of the design.

We next consider an example to illustrate the method.

Example 13: The filter specification corresponding to a fan filter is given by

$$\begin{aligned} P_d(\underline{\theta}) &= 1, \quad |\theta_1| \geq 3|\theta_2|, \quad -\pi \leq \theta_i \leq \pi, \quad i = 1, 2 \\ &= 0, \quad |\theta_1| < 3|\theta_2|, \quad -\pi \leq \theta_i \leq \pi, \quad i = 1, 2 \end{aligned}$$

This response (shown in Figure 16 on page 22) possesses quadrantal symmetry.

Here, we shall decompose this response into two components: one having symmetry about the $x_1 = x_2$ diagonal, and the other having antisymmetry about the same diagonal. Thus, the T operation used here is:

$$T = T_3 = \begin{bmatrix} 0 & 1 \\ 1 & 0 \end{bmatrix}$$

Applying Theorem 12, we get:

$$P_d(\underline{\theta}) = P_{d+}(\underline{\theta}) + P_{d-}(\underline{\theta})$$

where $P_{d+}(\theta_1, \theta_2) = \frac{1}{2} \cdot [P_d(\theta_1, \theta_2) + P(\theta_2, \theta_1)]$
and $P_{d-}(\theta_1, \theta_2) = \frac{1}{2} \cdot [P_d(\theta_1, \theta_2) - P(\theta_2, \theta_1)]$.

Using the above decomposition, we obtain (for $-\pi \leq \theta_i \leq \pi, i = 1, 2$):

$$\begin{aligned} P_{d+}(\underline{\theta}) &= 0.5, \quad |\theta_1| \geq 3|\theta_2| \cup |\theta_2| \geq 3|\theta_1| \\ &= 0, \quad |\theta_1| < 3|\theta_2| \cap |\theta_2| < 3|\theta_1| \end{aligned}$$

$$\begin{aligned} P_{d-}(\underline{\theta}) &= 0.5, \quad |\theta_1| \geq 3|\theta_2| \\ &= -0.5, \quad |\theta_2| \geq 3|\theta_1| \\ &= 0, \quad |\theta_1| < 3|\theta_2| \cap |\theta_2| < 3|\theta_1| \end{aligned}$$

The responses of $P_{d+}(\underline{\theta})$ and $P_{d-}(\underline{\theta})$ are shown in Figures 17 and 18, respectively, on pages 23 and 24. $P_{d+}(\underline{\theta})$ possesses octagonal symmetry and $P_{d-}(\underline{\theta})$ possesses octagonal antisymmetry. We next design these two components using optimization.

For $P_{d+}(\underline{\theta})$, which has octagonal symmetry, we know from Table 8 that $a_{kl} = a_{lk}$ and $b_{mn} = 0$. So assuming a impulse response size of 5×5 for our filter, its frequency response function will be:

$$P_+(\theta_1, \theta_2) = \sum_{k=0}^{2}\sum_{l=0}^{2} a_{kl} \cdot (\cos\theta_1)^k \cdot (\cos\theta_2)^l$$
$$\text{with } a_{kl} = a_{lk}.$$

Hence, there are 6 independent coefficients here. These coefficients are determined by minimizing the objective function:

$$J_+ = \sum\sum [P_+(\theta_1, \theta_2) - P_{d+}(\theta_1, \theta_2)]^2$$

The optimization required 129 function evaluations. The following are the optimized coefficients. The contour and 3-D plots are shown in Figure 19 on page 25.

$a_{00} = -0.07304$
$a_{01} = 0.1184$
$a_{02} = 0.4669$
$a_{10} = 0.1184$
$a_{11} = -0.2486$
$a_{12} = -0.02676$
$a_{20} = 0.4669$
$a_{21} = -0.02676$
$a_{22} = -0.5287$

Next, we design the component, $P_{d-}(\underline{\theta})$, which possesses octagonal antisymmetry of type 2 in Table 8. So, the frequency response function will be:

$$P_-(\theta_1, \theta_2) = \sum_{k=0}^{2}\sum_{l=0}^{2} \alpha_{kl} \cdot (\cos\theta_1)^k \cdot (\cos\theta_2)^l,$$
$$\text{with } \alpha_{kl} = -\alpha_{lk} \text{ and } \alpha_{kk} = 0$$

Here there are 3 independent parameters, which are determined by minimizing the objective function

$$J_- = \sum\sum [P_-(\theta_1, \theta_2) - P_{d-}(\theta_1, \theta_2)]^2$$

The optimization required 60 function evaluations. The optimized parameters are given below and the resulting contour and 3-D plots are shown in Figure 20 on page 28.

$a_{00} = 0$
$a_{01} = 0.3612$
$a_{02} = 0.1949$
$a_{10} = -0.3612$
$a_{11} = 0$
$a_{12} = 0.09579$
$a_{20} = -0.1949$
$a_{21} = -0.09579$
$a_{22} = 0$

The total frequency response function is obtained by adding $P_+(\theta_1, \theta_2)$ and $P_-(\theta_1, \theta_2)$, i.e.,

$$P(\theta_1, \theta_2) = P_+(\theta_1, \theta_2) + P_-(\theta_1, \theta_2)$$

The resulting contour and 3-D plots are given in Figure 21 on page 28.

So, by using decomposition, the design required $129 + 60 = 189$ function evaluations to determine a total of 9 independent parameters. In comparison, the design without decomposition is found to require 246 function evaluations to determine 9 independent parameters. So the advantage of using decomposition is clearly shown in the example.

Conclusion

The objective of this paper is to present the various results available in the literature on the symmetries and their applications for two-dimensional signals and systems. Specifically, a unified way of expressing the various commonly occurring symmetries is first presented and then the interdependencies resulting from various symmetries on signals and their Fourier transforms are developed using the unified symmetry representation. The application of symmetry conditions to speed up the fast Fourier transform algorithms is then discussed. Analysis of the magnitude responses of filters shows that utilization of their symmetries will considerably simplify the complexity of the design and implementation of these filters. Finally, techniques for the application of symmetry results even for functions that do not possess symmetries by using symmetrical decomposition are presented. The various results and techniques presented in this paper show that a knowledge and application of the various symmetries in the responses of 2-D systems will considerably reduce the complexity of the design and implementation of these systems. Symmetry with complex polynomials will also provide similar advantage. Further, it may be noted that symmetry results can be extended to three and higher dimensional systems [29, 30]. Although the paper dealt with the symmetry in magnitude func-

tion, similar advantages can be obtained by identifying phase symmetries. Due to lack of space these are not presented in this paper. The more recent research in the symmetry theory and its application to 2-D filter design is through the use of the delta operator. The main advantage with regard to the theory is that it unifies the results of 2-D analog and discrete-time case. From the point of view of design, there is a major advantage in the coefficient sensitivity for narrowband filters [31–36].

References

[1] J. Rosen, *Symmetry Discovered*. Cambridge, England: Cambridge University Press. 1975.

[2] A.V. Shubinov and V.M. Koptsik, *Symmetry in Science and Art*. New York: Plenum Press. 1974.

[3] A. Fettweis, "Symmetry requirements for multidimensional digital filters," *Int. Journal Circuit Theory Appl.*, vol. 5, pp. 343–353, 1977.

[4] M. Narasimha and A. Peterson, "On using symmetry of FIR filters for digital interpolation," *IEEE Tran. Acoust., Speech, Signal Processing*, vol. ASSP-26, pp. 267–268, 1978.

[5] P. K. Rajan and M.N.S. Swamy, "Symmetry conditions on two-dimensional half-plane digital filter transfer functions," *IEEE Trans. Acoust., Speech, Signal Processing*, vol. ASSP-27, pp. 506–511, October 1979.

[6] D.M. Goodman, "Symmetry Conditions for Two-dimensional FIR Filters", *Lawerence Livermore Lab Rep*. UCID-311, 1979.

[7] S.A.H. Aly, J. Lodge and M.M. Fahmy, "The design of two-dimensional digital filters with symmetrical or anti-symmetrical specifications," *Proc. 1980 Eur. Conf Circuit Theory Des.*, Warsaw, pp. 145–150, 1980.

[8] D.M. Goodman, "Quadrantal symmetry calculations for nonsymmetric half-plane filters," *Proc. 14th Asilomar Conf*, vol. 14, 1980.

[9] S.A.H. Aly and M.M. Fahmy, "Symmetry exploitation in the design and implementation of two-dimensional rectangularly sampled filters," *IEEE Trans. Acoust., Speech, Signal Processing,* vol. ASSP-29, pp. 973–982, 1981.

[10] J.H. Lodge and M.M. Fahmy, "K-cyclic symmetries in multidimensional sampled signals," *IEEE Trans. Acoust., Speech, Signal Processing,* vol. ASSP-31, pp. 847–860, 1983.

[11] D.E. Dudgeon and R.M. Merserau, *Multidimensional Digital Signal Processing*. Englewood Cliffs, NJ: Prentice-Hall, 1984.

[12] B.P. George and A.N. Venetsanopoulos, "Design of two-dimensional recursive digital filters on the basis of quadrantal and octagonal symmetry," *Circuits Syst. Signal Processing,* vol. 3, pp. 59–78, 1984.

[13] J. Pitas and A.N. Venetsanopoulos, "The use of symmetries in the design of multidimensional digital filters," *IEEE Trans. Circuits Syst.,* vol. CAS-33, pp. 863–873, 1986.

[14] A. Fettweis, "Multidimensional digital filters with closed loss behavior designed by complex network theory approach," *IEEE Trans. Circuits Syst.,* vol. CAS-34, pp. 338–344, 1987.

[15] P.K. Rajan and M.N.S. Swamy, "Quadrantal symmetry associated with two-dimensional digital filter transfer functions", *IEEE Trans. Circuits Syst.,* vol. CAS-25, pp. 340–343, June 1978.

[16] P.K. Rajan, H.C. Reddy, and M.N.S. Swamy, "Further results on 4-fold rotational symmetry in 2-D functions", *Proc. 1982 IEEE Int. Conf. Acoust., Speech, Signal Processing, Paris.* May 1982.

[17] P.K. Rajan, H.C. Reddy and M.N.S. Swamy, "Fourfold rotational symmetry in two-dimensional functions", *IEEE Trans. Acoust., Speech, Signal Processing.* vol. ASSP-30, pp. 488–499, June 1982.

[18] V. Rajaravivarma, P.K. Rajan and H.C. Reddy, "Symmetry study on 2-D complex analog and digital filter functions," *Multidimensional Systems and Signal Processing,* vol. 2, pp. 161–187, 1991.

[19] M.N.S. Swamy and P.K. Rajan, "Symmetry in 2-D filters and its application," in *Multidimensional Systems: Techniques and Applications* S.G. Tzafestas, Ed. New York: Marcel Dekker, 1986, Ch. 9.

[20] H.C. Reddy, I.H. Khoo and P.K. Rajan, "Symmetry and 2-D Filter Design", *The Circuits and Filters Handbook* W. K. Chen, Ed. Boca Raton, FL: CRC Press, 2002.

[21] H. Weyl, *Symmetry*. Princeton: Princeton University Press, 1952.

[22] P.K. Rajan, H.C. Reddy, M.N.S. Swamy, "Symmetry relations in two-dimensional fourier transforms," in *Proc. 1984 IEEE-ISCAS*, vol. 3, pp 1022–1025, 1984.

[23] G.A. Bliss, *Algebraic Functions*. New York: Dover, 1966.

[24] P.K. Rajan, H.C. Reddy, "A test procedure for 2-D discrete scattering Hurwitz polynomials," *IEEE Transactions on Acoustics, Speech and Signal Processing,* vol. ASSP-37, pp. 118–120, January 1989.

[25] H.C. Reddy, P.K. Rajan, "A comprehensive study of two-variable Hurwitz polynomials," *IEEE-Trans. on Education,* pp. 198–209, Aug. 1989.

[26] H.C. Reddy, "Theory of two-timensional Hurwitz polynomials," *The Circuits and Filters Handbook* W. K. Chen, Ed. Boca Raton, FL: CRC Press, 2002.

[27] P.K. Rajan and H.C. Reddy, "Symmetrical decomposition and Transformation," *Mathematics and Computers in Simulation,* vol. 27, no 5/6, pp. 585–598, Oct. 1985.

[28] V. Rajaravivarma, P.K. Rajan and H.C. Reddy, "Design of multidimensional FIR digital filters using symmetrical decomposition technique," *IEEE Transactions on Signal Processing,* vol. 42, no. 1, pp. 164–174, Jan. '94.

[29] V. Rajaravivarma, P.K. Rajan, H.C. Reddy, "Study of phase symmetry in 3-D filters," *Proc. Southeast Conference 1989*, Columbia, South Carolina, April 1989.

[30] V. Rajaravivarma, P.K. Rajan, H.C. Reddy, "Planar symmetries in 3-D filter responses and their application in 3-D filter design," *IEEE Transactions on Circuits and Systems II*, vol. 39. no. 6, pp 356–368, June 1992.

[31] H.C. Reddy, P.K. Rajan, G.S. Moschytz and A.R. Stubberud, "Study of various symmetries in the frequency response of two-dimensional delta operator formulated discrete-time systems," *Proc. 1996 IEEE-ISCAS,* vol. 2, pp. 344–347, May 1996.

[32] H.C. Reddy, I.H. Khoo, G.S. Moschytz and A.R Stubberud, "Theory and test procedure for symmetries in the frequency response of complex two-dimensional delta operator formulated discrete-time systems," *Proc. the 1997 IEEE-ISCAS,* vol. 4, pp. 2373–2376, June 1997.

[33] H.C. Reddy, I.H. Khoo, P.K. Rajan, "Symmetry in the frequency response of two-dimensional delta operator formulated discrete-time systems," *Proc. the 1997 ECCTD,* vol. 3, pp. 1118–1123, Aug 1997.

[34] H.C. Reddy, I.H. Khoo, P.K. Rajan and A.R. Stubberud, "Symmetry in the frequency response of two-dimensional (γ_1, γ_2) complex plane discrete-time systems," *Proc. 1998 IEEE-ISCAS,* vol. 5, pp. 66–69, May 1998.

[35] I.H. Khoo, H.C. Reddy and P.K. Rajan, "Delta operator based 2-D filter design using symmetry constraints," *Proc. 2001 IEEE-ISCAS,* vol. 2, pp 781–784, May 2001.

[36] I.H. Khoo, H.C. Reddy and P.K. Rajan, "Delta operator based 2-D filters: Symmetry, stability, and design," *Proc. 2003 IEEE-ISCAS,* May 2003.

Hari C. Reddy received the B.E. degree in electrical engineering in 1964 from Sri Venkateswara University, Tirupati, India; the M.E. degree in electrical engineering from M.S. University of Baroda, Baroda, India in 1966; and the Ph.D. degree in electronics and communication engineering, from Osmania University, Hyderabad, India in 1974. He then did two years of post doctoral research work at the Concordia University, Montreal, Canada, 1975–1977.

Professor Reddy has been with the Department of Electrical Engineering, California State University, Long Beach (CSULB), as a tenured professor since 1987. Dr. Reddy was with the Department of Electrical Engineering at Tennessee Technological University, Cookeville, Tennessee associate professor from 1980–1983 and as tenured professor from 1983–1987. Before joining Tennessee Tech, Dr. Reddy held teaching and research positions at the State University of New York College at Buffalo; Concordia University, Montreal, Canada; Osma-

nia University, Hyderabad India; and S.G.S. Institute of Science and Technology, Indore, India.

During the past ten years he has been guest professor at the Institute for Signal and Information Processing and Institute for Integrated Systems, Swiss Federal Institute of Technology (ETH) Zurich, Switzerland; and visiting researcher from 1994 to 1999 in the Department of Electrical and Computer Engineering at the University of California, Irvine, California.

Dr. Reddy's teaching and research interests are in the broad areas of circuit design, filters, systems and signal processing. His research is concerned with the theory and applications of multidimensional circuits, systems and digital filters. For the past several years, he has also been working on the development of circuit theory for high speed signal processing and other related problems using the delta discrete time operator. He has co-authored about one hundred and twenty five research papers and three book chapters. He attended and presented papers in over fifty international conferences.

Dr. Reddy has been interested on the impact of advances of research on electrical engineering education. He was guest editor for the special issue on research and education—circuits and systems of the *IEEE Transactions on Education* published in August 1989. He served as principal associate editor for the *IEEE Transactions on Education* (1984–1990). From 1993 to 1996, he was also associate editor for *IEEE Transactions on Circuits and Systems (Part I)* and also served as associate editor for the *Journal of Circuits, Systems and Computers*. In 1999, he co-organized and served as general chair of the IEEE CAS Society's 3rd Emerging Technologies Workshop on Mixed Signal Integrated Circuit Design held in Long Beach, California.

Professor Reddy served as president-elect, president and past president of the IEEE Circuits and Systems Society (CASS) in 2000, 2001 and 2002 respectively. Earlier, he served as CASS vice president for conferences for three years (1996, 1997, 1999). From 1993 to 1995, he was a member of the CASS Board of Governors.

Prof. Reddy is a recipient of the 2003 IEEE Circuits and Systems Society's Meritorious Service Award. Also, in 2003, Prof. Reddy received the diploma of honorary member of the Senate of the Technical University of Iasi, Romania and the "Gh. Asachi" University Medal for outstanding contributions in the activities of cooperation with the faculties of the Technical University. Prof. Reddy was elected as a Fellow of the IEEE in 1992 for contributions in the field of multidimensional circuits and systems.

Prof. Reddy is a recipient of the Distinguished Faculty Scholarly and Creative Achievement Award (1990) and the Outstanding Professor Award (1993) from the California State University at Long Beach. He received (at the 1990 and 1992 Commencements) the TRW Excellence in Research and Teaching Awards.

I-Hung Khoo received the B.S. and M.S. degrees from the California State University, Long Beach in 1990 and 1996 respectively, and the Ph.D. degree from the University of California, Irvine in 2002. He is currently a postdoctoral researcher at the University of California, Irvine. His research interests include analog and digital signal processing, and mixed-signal integrated circuit design.

P. K. (Kari) Rajan received the B.E. degree from the University of Madras in 1966 and M.Tech. and Ph.D. degrees in electrical engineering from the Indian Institute of Technology, Madras, in 1969 and 1975 respectively. He spent about two years as a post doctoral fellow at the Concordia University, Montreal, two years as assistant professor at the SUNY College of Technology, Buffalo, New York, and three years as associate professor at the North Dakota State University, Fargo, North Dakota. He joined the Tennessee Technological University in 1983 as associate professor and since 1992 has served as professor and chair of the Department of Electrical and Computer Engineering.

Dr. Rajan's areas of teaching and research interests are circuits, systems and signal processing. He has published over one hundred articles in refereed journals and conference proceedings. He has co-authored two book chapters. He was elected a Fellow of IEEE in 1995 for his contributions research and teaching in multidimensional circuit theory and signal processing. He has served as associate editor of the *IEEE Transactions on Circuits and Systems* and the *IEEE Transactions on Education*. He is serving as associate editor for the journal *Multidimensional Systems and Signal Processing*.